RHEOLOGICAL BEHAVIOR OF CARBON BLACK INKS

A Thesis Submitted to
the Graduate School of Engineering and Sciences of
İzmir Institute of Technology
in Partial Fulfillment of the Requirements for the Degree of

MASTER OF SCIENCE

in Chemical Engineering

by
Deniz EKERLER

January 2022
İZMİR

ACKNOWLEDGEMENTS

I would like to express my gratitude in the first place to my advisor Prof. Dr. Muhsin ÇİFTÇİOĞLU for the useful comments, remarks and engagement through the learning process of this master thesis.

I would like to acknowledge and thank Dr. Özlem DUVARCI for precious help, advice, valuable comment, and contributions. I learned many things regarding rheology with her helps.

I would like to thank SUN CHEMICAL management for their understanding and support to obtain my MSc degree. I would also like to express my gratitude to my managers Serkan SAYGI and Serdar ÖZER for their support and understanding despite the heavy workload in the factory in receiving my master's degree.

Special thanks to my colleague and friend Seda Sultan YÜKSEL for endless understanding. This thesis work would not have been possible without her help and encouragement.

I am most grateful to my dear family Latif and Şefika EKERLER for their eternal support, never ending love and encouragement during my education life.

ABSTRACT

RHEOLOGICAL BEHAVIOUR OF CARBON BLACK INKS

The printing ink industry is increasingly facing challenges in terms of high manufacturing costs and quality requirements. Rheological properties of the inks must be better understood for the development of production and application processes. Effects of pigment and dispersant content, varnish/solvent ratio, grinding medium, grinding time and storage period on rheological and printed optical properties were investigated for carbon black inks in this thesis work.

The viscosity of the dispersant free ink was higher than inks with dispersant. The viscosity of the dispersant-free ink increased after three months storage whereas the viscosity of the dispersant-containing ink remained almost constant. Pigment content or V/S ratio increase resulted in higher viscosities. Grinding with 0.5 mm beads provided a finer size distribution and lower viscosities than ink ground with 0.8 mm beads. Longer grinding time increased the ink viscosities at pigment contents over 20 wt%.

Thixotropy of dispersant free ink was determined to be about 12 times higher than 0.5 wt% dispersant containing ink. The thixotropy area of the 30 wt% pigment containing ink was determined to be five times higher than that of 25 wt% pigment containing ink. The thixotropy of the 25 wt% pigmented ink increased when the grinding time was changed from 30 to 60 minutes. Inks with coarser particle size distribution had higher thixotropy.

Loss tangent (G''/G') at 10 Hz was used to create a correlation with color strength. Color strength of 14 out of 16 inks was determined higher with lower loss tangent values. Inks containing dispersant, higher pigment contents, varnish/solvent ratios close to one, increasing grinding time at higher pigment content increased the color strengths in printings.

ÖZET

KARBON KARASI MÜREKKEPLERİN REOLOJİK DAVRANIŞLARI

Mürekkep endüstrisi yüksek üretim maliyetleri ve kalite gereksinimleri sebebiyle giderek artan zorluklarla karşılaşmaktadır. Mürekkeplerin reolojik özellikleri, mürekkep üretim ve uygulama proseslerinin geliştirilmesi için, daha iyi anlaşılmalıdır. Bu tez çalışmasında, pigment oranı, dağıtıcı oranı, vernik/çözücü oranı, öğütme ortamı, ezme süresi ve saklama periyodunun hem reolojik hem de basılmış optik özellikler üzerindeki etkileri karbon karası mürekkepler için araştırıldı.

Dağıtıcı içeriğinin arttırılmasıyla, mürekkeplerin viskozitesi düştü ve kayma hızı arttıkça viskozitesi azaldı. Dağıtıcı içermeyen mürekkebin viskozitesi üç aylık depolamadan sonra arttı halbuki dağıtıcı içeren dispersiyonun viskozitesi yaklaşık sabit kaldı. Pigment içeriği veya V/S oranı artışı, daha yüksek viskozitelerle sonuçlandı. 0.5 mm'lik bilyeler ile ezme, 0.8 mm'lik bilyelerle ezmeye göre daha ince boyut dağılımı ve daha düşük viskozite sağladı. Daha fazla ezme süresi kütlece % 20'den yüksek pigment oranlarında viskoziteyi arttırdı.

Dağıtıcı içermeyen mürekkebin tiksotropisinin, ağırlıkça % 0.5 dağıtıcı içerene göre 10 kat daha yüksek olduğu belirlendi. Ağırlıkça % 30 pigment içeren mürekkebin tiksotropik alanının, ağırlıkça %25 pigment içeren mürekkebe göre beş kat daha yüksek olduğu belirlendi. Ağırlıkça %25 pigment içeren mürekkebin tiksotropisi, öğütme süresi 30 dakikadan 60 dakikaya çıkarıldığında arttı. Daha büyük partikül boyutu dağılımına sahip mürekkepler daha yüksek tiksotropiye sahipti.

Renk şiddeti ile bir korelasyon oluşturmak için 10 Hz'deki kayıp tanjantı (G"/G') kullanıldı. 16 mürekkepten 14'ünün renk şiddeti, daha düşük kayıp tanjant değerleriyle daha yüksek olarak belirlendi. Dispersant içeren mürekkepler, daha yüksek pigment içeriği, bire yakın vernik/solvent oranları, daha yüksek pigment içeriğinde öğütme süresinin artması baskılarda renk kuvvetlerini artırdı.

TABLE OF CONTENTS

LIST OF FIGURES

Figure **Page**

Figure **Page**

Figure **Page**

LIST OF TABLES

Table **Page**

LIST OF SYMBOLS/ABBREVIATIONS

f	Frequency
G′	elastic/storage modulus
G″	viscous/loss modulus
G*	complex modulus
LVER	Linear viscoelastic region
t	time

Greek Letters

γ	shear strain
τ	shear stress
τo	yield stress/ applies stress (constant)
$\dot{\gamma}$	Shear rate
τ	shear stress
η	viscosity
η_o	zero shear viscosity
η_∞	infinite shear viscosity
ω	radial frequency
δ	shift angle

CHAPTER 1

INTRODUCTON

Inks are composed of pigments, resins, solvents and dispersants. Inks are mainly stable pigment particle dispersions in liquid medium. Pigments are used for imparting color to inks and application surfaces. Resins are responsible from adherence of ink film to the applied substrate. Solvents provide the liquid medium responsible for film formation and drying requirements of inks. Dispersants generally adsorb on pigment particles and regulate interactions between particles and the liquid medium.

Carbon black pigments are produced by partial combustion of hydrocarbons. Carbon black pigment is mainly used as reinforcing agent in rubbers for tires and other rubber groups. Carbon black pigment is also used in printing inks and coatings due to strong hiding power and light absorption. Color properties of carbon black pigments depend on particle size distribution, morphology and structure (Barrie et al., 2004). High surface area of carbon black pigments create difficulties in dispersion quality (Nsib et al., 2006).

Printing ink industry is one of the growing markets due to the increase of end-use products, flexible packaging, labels, and publishing. Quality of inks is dictated by the level of pigment dispersion which can be divided into three main stages which are wetting, grinding and stabilization. Wetting is replacement of pigment/air interface with pigment/liquid medium interface. Break up of pigment powders or agglomerates into smaller particles is accomplished during grinding. Grinding process is affected by stirring speed, stirrer type, grinding medium bead size, filling ratio of grinding chamber. Stabilization is the sufficient separation of pigment particles from each other so that the repulsive forces exceed the attractive forces. Agglomerate formation starts when attractive forces become higher than repulsive forces. Agglomerates deteriorate the rheological properties and printing performance of inks.

Rheology is study of deformation and flow. Rheological properties of dispersions are impacted by pigment particle size, shape and concentration (Barrie et al., 2004). Rheological behavior of inks is characterized by the determination of both steady

(viscosity, thixotropy, yield point) and dynamic shear properties (viscous and elastic). Rheological behavior mainly depends on the relation between shear rate and shear stress.

Generally, inks have a Non-Newtonian behavior due to relatively high pigment contents. Non-Newtonian inks are subdivided into three types as pseudoplastic, dilatant and plastic. Dynamic shear properties of dispersions show structural interactions of solvent, binder, pigments and important for the development of desired application properties. Dynamic shear rheology can be measured with creep test, oscillatory test, stress relaxation test and start up test by using a rheometer. Oscillatory tests (amplitude and frequency sweep) are mostly used for dynamic shear rheology characterization.

Rheological behavior of ink affects application quality. Characterization and manipulation of dispersion rheology can provide optimal processing and application performance. Ink rheology affects ink transfer during the printing process and application properties. Correlation between ink rheology and printing properties must be understood for obtaining high quality films.

Observed colors are a result of interactions of light and surfaces. Pigments absorb and scatter certain components of light to form colors. Importance of colors is increasing in our daily life and directing customers' purchasing behavior. Brands try to create recognizable and consistent colors that speak about their identity. Importance of color creates more demands regarding specifications of both inks and prints. Printed products are assessed according to optical properties of printed surfaces. Color strength is an important optical property of an ink that is described as the ability to keep printed surface colored.

This thesis work was focused on the effects of pigment content, dispersant ratio, varnish/solvent ratio, grinding medium, grinding time and storage duration on rheological behavior of carbon black inks and tried to correlate them with printing performances.

CHAPTER 2

PIGMENT DISPERSION

Pigments are widely used in various industries like plastics, cosmetics, pharmaceutical, paints, and inks. Among various chemical and physical properties, pigments are mainly selected for their colors and classified according to their chemical structure as organic or inorganic. Organic pigments provide better color properties than inorganic pigments due to their morphology and molecular structure (Christiana et al., 2017).

Solvent-based inks are formulated by using various components like organic solvents, binders, pigments, surfactants, dispersants and rheology modifiers. Resins in ink formulation are responsible from the cross-linking network structure and bind ink to the substrate surface. Solvents in formulation are designed to dissolve resin and enhance flow properties. Inks are produced by dispersing of pigment particles in a liquid medium. Dispersion process can be defined to occur in three main stages which are wetting, disruption, and stabilization as schematically shown in Figure 2.1. The aim of pigment dispersion process is to produce stable and uniform pigment suspensions which is vital for commercial ink applications.

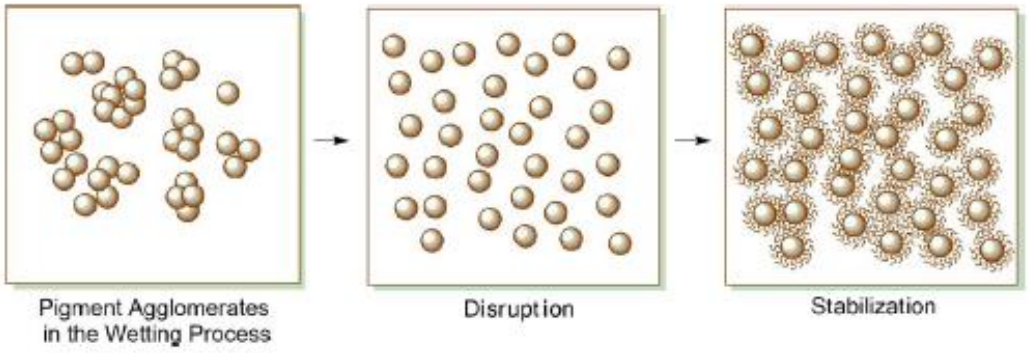

Figure 2.1. Dispersion process

(Source: Agbo et al., 2017)

First step in dispersion process is wetting of pigment particles. Wetting is replacement of pigment/air interface with pigment/liquid medium interface. Shear forces

applied to pigment-binder-solvent mixture enhance interaction between pigment surface and binder. Main parameters that have effect on wetting are particle geometry, viscosity of medium, surface tension of medium and chemical character of solvents. Wetting properties of titanium dioxide were investigated by analyzing wetting efficiency and deagglomeration process/energy. Particles with smaller sizes had lower wetting speed. There was an inverse proportional relationship between wetting speed and energy of deagglomeration; slower wetting speeds required higher energy for dispersion (Abrahao et al., 2013).

Deagglomeration of pigment particles is necessary until required level of dispersion is achieved after the wetting stage. Energy required for dispersion of particles is supplied by grinding machines or mixers and added energy separates pigment particles from each other. Energy supplied during the mixing/milling and its duration are critical parameters in obtaining the desired level of dispersion.

Pigments and other components/species in the ink dispersions have a rather complicated combination of repulsive and attractive interactions with each other. Pigment particles can be stabilized by the breakdown of pigment agglomerates/aggregates which can only be possible if repulsive forces between them are higher than attractive forces. Electrostatic Stabilization and Steric Stabilization are commonly known to be the two main mechanisms for stabilization of pigment particles in dispersions. Electrostatic stabilization becomes dominant when particles having surface charges or adsorbed charged dispersants encounter other charged particles. When charged particles approach each other in dispersion, charged layers start to overlap and repulsion occurs.

Adsorption of nonionic surfactant or polymer layers of A-B, A-B-A on particle surfaces provides steric interaction between particles. B part of the polymer is “anchor” chain with high affinity to adsorb on particle surface, while A part is “stabilizing” chain that is soluble in medium. When particles with adsorbed polymer approach each other, polymer layers start to interact with each other. Two particles with adsorbed polymer layers will repel each other when these layers interact with each other. Steric stabilization is schematically shown in Figure 2.2 (Oyarzún et al., 2015).

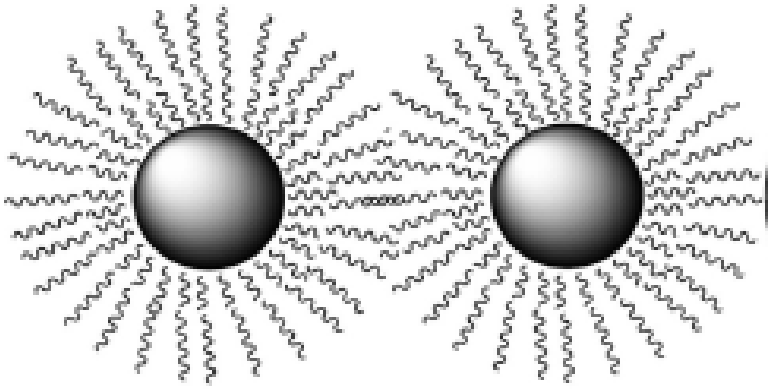

Figure 2.2. Steric Stabilization

(Source: Oyarzún, 2015)

Dispersions have small particles that undergo Brownian motion while they may collide with each other. During collisions, particles approach each other in nanometer scale distances which may cause agglomeration of particles due to the formation of attractive forces. Van der Waals forces, London forces, Coulombic forces and hydrogen bonds are major links between pigment particles and have impact on formation of instability.

Interaction of particles in dispersion can cause stability or instability. Dispersed particles are thermodynamically unstable, and they have tendency to reach lower energy state when linking together. DLVO theory (named for the theorist Derjaguin, Landau, Verway and Overbeek) describes dispersion stability in terms of the total potential energy (Gt) which is the sum of attractive energy (Ga) and repulsive energy (Ge) at various distances. Figure 2.3 shows behavior of Gt with distance (h) between particles and this relation is shown below:

$$Gt = Ge + Ga \qquad (2.1)$$

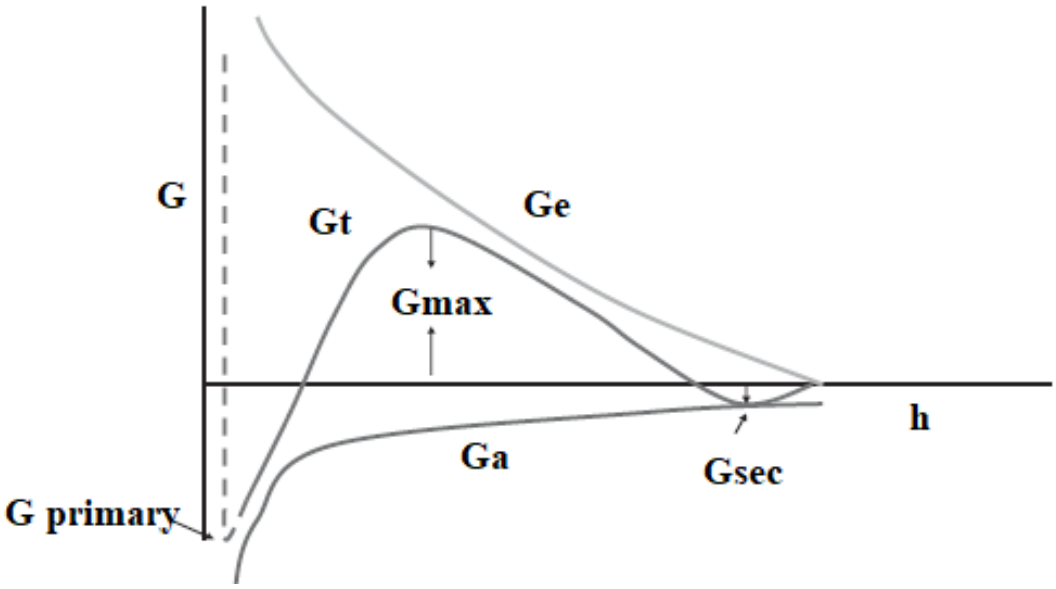

Figure 2.3. Variation of Gt with h according to DLVO theory.

(Source: Tadros, 2010)

Ge decays with increasing interparticle distance, but Ga changes inversely with square of the distance. There are two minimum and one maximum point in Gt-h graph. Ga>Ge at high distances and this forms a secondary minimum, this area could form weak and reversible aggregates. At very small interparticle distances Ga >> Ge where primary minimum is formed and at that point strong aggregation can occur.

Particles repel each other and form a stable dispersion when repulsive forces dominate. Particles form bonds with each other and form aggregates which causes the occurrence of an unstable dispersion when attractive forces are higher than repulsive forces. Initially dimers and trimers will form and after a while particles form agglomerates/aggregates. Sedimentation will occur when the sizes of these agglomerates/flocculates exceed a certain range. Figure 2.4 shows stable, early flocculation, unstable and sedimentation stages of a dispersion.

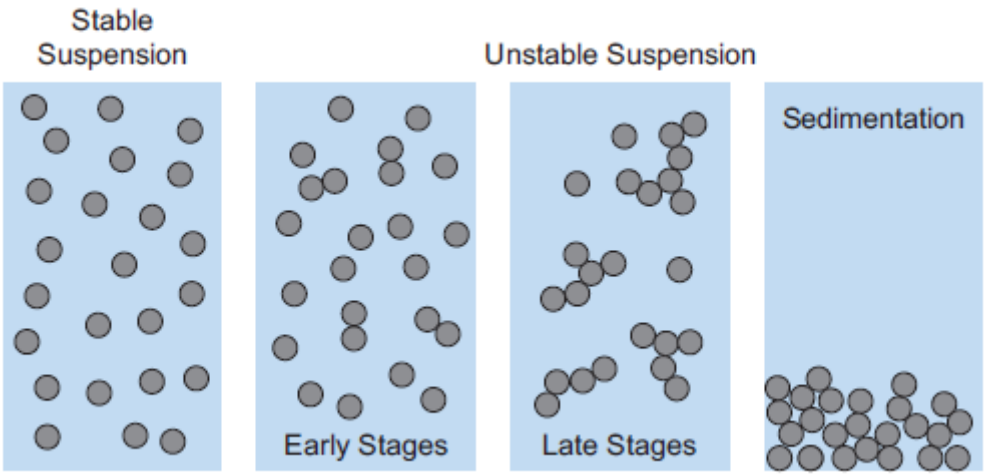

Figure 2.4. Shematic representation of dispersion microstructure and interparticle forces

(Source: Trefalt & Borkovec, 2014)

The nature of the interparticle forces mainly is responsible from the rheological and various application related properties of dispersions. Dispersion and stability of pigment particles are important for many applications however it has highest effect on rheological behavior/characteristics and structure of the suspensions. (Pal & Fleming, 2006)

CHAPTER 3

RHEOLOGICAL BEHAVIOR OF DISPERSIONS

Rheology has been appropriately defined as the investigation of the flow and deformation of materials. The dispersion rheological behavior play a vital role in many industrial applications (like paint, ink, ceramic, cosmetic, pharmaceutical, food etc.). The control of rheological behavior is necessary for satisfactory production and application processes. Understanding microstructure and flow pattern of dispersion is essential for controlling rheological behavior.

Ideal solids deform elastically under stress. Energy required for deformation is recovered when stress is removed. Ideal fluids deform irreversibly and when applied shear is removed that energy can't be recovered due to dissipation of energy within the fluid as heat. Most of materials like dispersions are classified between these two opposite extremes.

Parallel plate model is helpful to explain shear stress and shear strain terms. The model description involves two parallel plates where one is stationary and the other one moves with force and interceding area is filled with fluid as shown in Figure 3.1. Force applied to the upper plate with area A starts moving the upper plate and leads to the flow of liquid in contact with that plate. Force applied to the upper plate per unit area is called as shear stress as given below:

$$\tau = F/A \qquad \text{The unit of the shear stress is [Pa]} \qquad (3.1)$$

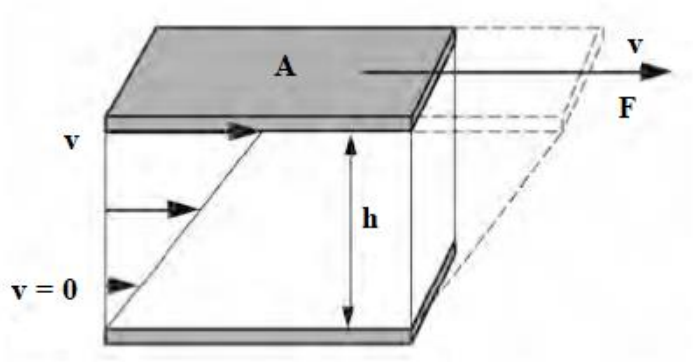

Figure 3.1. The Two-Plates-Model for shear tests to illustrate the velocity distribution of a flowing fluid in the shear gap

(Source: Mezger, 2014)

Applied shear stress causes flow of fluid and maximum flow speed V_{max} is found close to the upper plate. Between gap of "h" speed drops to zero close to the stationary plate and a velocity gradient forms between plates. This velocity gradient is called as shear rate as expressed by the following equation:

$$\dot{\gamma} = v/h \qquad \text{Unit of the shear rate is } [s^{-1}] \qquad (3.2)$$

The rheological properties can be assessed by determining the steady state (e.g viscosity, yield stress, thixotropy) and dynamic state (elastic and viscous modulus) properties of the inks which straightforwardly affect application and production.

3.1. Steady-state properties of inks

3.1.1. Viscosity

Viscosity is a steady state property of a fluid. Molecules in a fluid show a relative motion between each other and these motions generate some internal frictional forces. Viscosity is defined as the resistance of liquid to flow and related with the internal friction

within the fluid. When a fluid starts to flow under the action of a force, flow resistance arises everywhere in the fluid that tends to oppose the motion. All fluids display a resistance against flow that can be defined as viscosity which is expressed as:

$$\eta = \tau / \dot{\gamma} \qquad \text{Unit of shear viscosity is [Pas]} \qquad (3.3)$$

Newtonian fluid is named after Sir Isaac Newton (1642 - 1726) who explained the behavior of flow with a linear equation between shear stress and shear rate. Newtonian fluids exhibit ideal fluid behavior and ratio of shear stress to shear rate is constant and viscosity does not change with deformation or time, varies only with pressure and temperature. Liquids having simple molecular structures like water, organic solvents have Newtonian behavior. Figure 3.2 shows the flow behavior of Newtonian fluids and their linear relationship between shear rate and shear stress. Slope of this curve gives viscosity of Newtonian fluid. Liquids with higher slopes of the flow curves have higher viscosities.

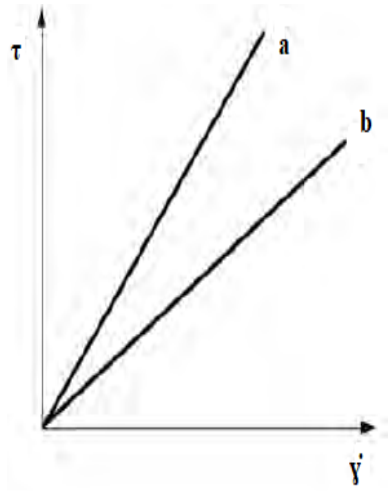

Figure 3.2. Flow curve of a Newtonian fluid

(Source: Mezger, 2014)

Fluids displaying non-linear relationship between shear stress and shear rate are called as non-Newtonian fluids. Most dispersions (except very dilute dispersions) do not behave like Newtonian fluids. The change in viscosity of non-Newtonian fluids with shear rate is shown in Figure 3.3 where various flow behaviors like (a) Newtonian; (b)

Bingham plastic; (c) Pseudoplastic (shear thinning); (d) Dilatant (shear thickening); and (e) Yield stress/shear thinning can be identified.

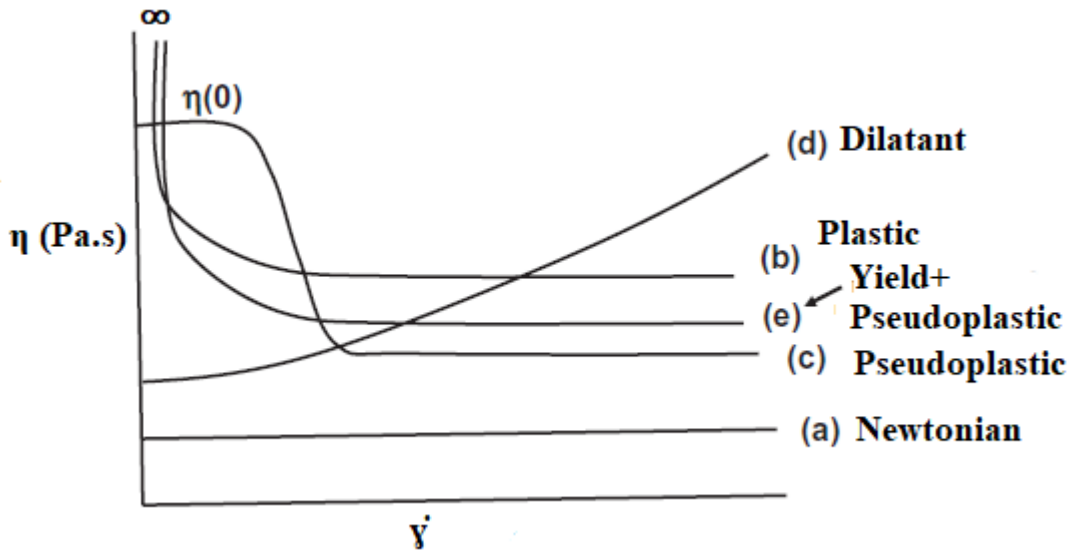

Figure 3.3. Rheological behavior of Non-Newtonian dispersions

(Source: Tadros, 2010)

Addition of solid particles to a Newtonian liquid leads to a significant deviation from Newtonian behavior. This deviation directly related with particle association and physical or chemical interactions. When shear rate increases in higher proportion than shear stress materials have a shear thinning or pseudo-plastic behavior. On the opposite side, when shear rate decreases in more proportion than shear stress, materials show shear thickening or dilatant behavior.

Viscosity of a shear thinning (pseudoplastic) liquid directly depends on applied shear rate or shear stress which means when more force is applied to material more mass can flow. Many dispersions have a shear thinning behavior. Structural changes in the dispersion with applied shear is shown in Figure 3.4. The components of the dispersion like polymer molecules or particles form an irregular internal order and this structure resist flow which yields a high viscosity at rest. Internal order and the orientation of particles will change in the direction of flow with increase in shear rate. Flow directed orientation will allow slip pass of particles easily. Shearing provides disintegration of

agglomerates and decrease of particle interactions, which results in easier flow of particles.

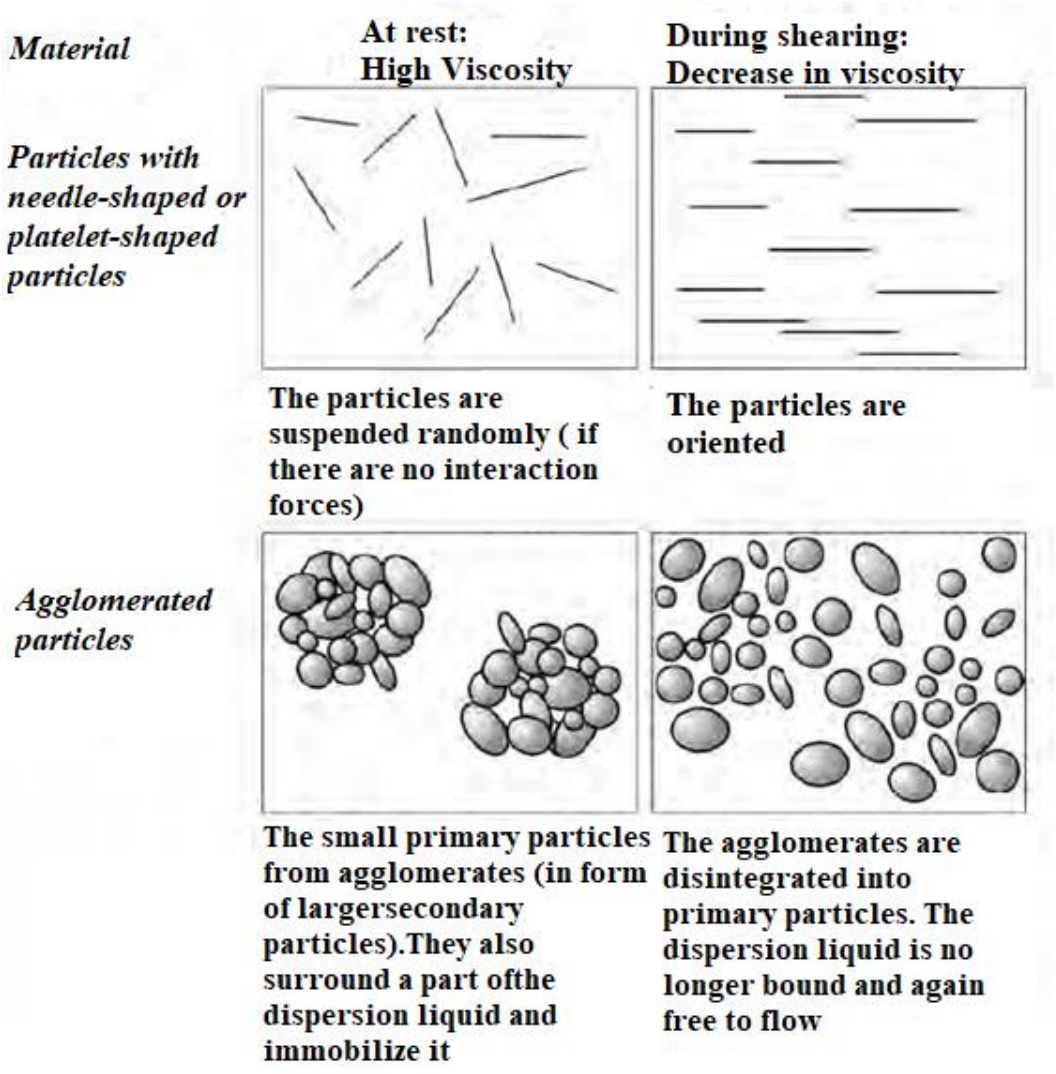

Figure 3.4. Structural changes in shear thinning behavior

(Source: Mezger, 2014)

Shear thinning behavior at low and high shear rates is not uniform and is shown in Figure 3.5. Brownian motion keeps particles in orientation or randomization during shearing at low shear rates and shear thinning dispersions behave like Newtonian with constant shear viscosity (η_0) as shown in region I. At high shear rates, shear induced forces exceed randomization effect of Brownian motion and viscosity will decrease. Viscosity will reach a finite constant value (η_∞) and further increase of shear rate will not

influence viscosity as shown in region III at very high shear rates. The structural orientation will be reconstituted through Brownian motion upon the reduction of shear in a certain time. This time dependent behavior will be discussed in more detail in the Thixotropy part later.

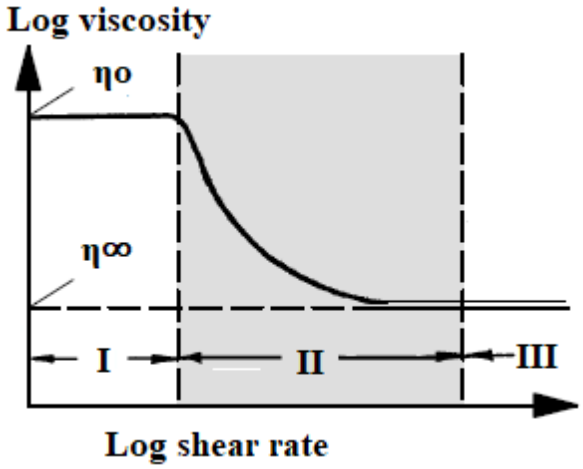

Figure 3.5. Shear thinning behavior

The viscosities of shear thickening (dilatant) materials increase with increasing shear rate. Dispersions having higher particle volume contents have shear thickening behavior at higher shear rates. This behavior is caused by the integration/formation of linkages/bonds between the particles which generates a flow resistance increase. Particle structure is broken down and instant particle clumps due to particle orientation are formed and these shear induced clumps cause volume increase during flow and increase viscosity at high shear rates.

Milling time effect on dispersion state and rheological behaviors of carbon nanotubes were investigated in a recent research article. Carbon nanotubes were ground at different milling times after premixing for 2, 5, 10, 15, and 20 h with yttria-stabilized zirconia beads and one sample was only premixed. All suspensions showed shear thinning behavior in the shear rate range of 0.1 s^{-1} to 1000 s^{-1}. Milled samples had higher starting viscosity than the sample only premixed. Among milled samples, 1 h ground dispersion had the highest viscosity over the entire shear rate range. After 1 h of milling, viscosity

decreased gradually. Grinding only 1 h was sufficient to separate particles from each other and formation of a dense network structure. On the other hand, grinding longer than 1 h affected bundle diameter and decreased viscosity (Kim et al., 2019).

Nsib et al. (2006) investigated the effect of two dispersants on dispersion of carbon black pigment in non-aqueous medium. Ester of hydroxy-carboxylic acid with lower molar mass and Alkyl ester of polycaprolactone with higher molar mass were used for investigation of dispersant effect and amount of required dispersant was optimized with rheological measurements. Shear thinning behavior was observed for samples containing low molar mass dispersant. This shear thinning behavior was directly related with limited deflocculation effect of low molar mass dispersant on pigment particles. Samples prepared with high molar mass dispersant showed a similar behavior to Newtonian fluids. Main reason behind that Newtonian like behavior was related with formation of thick layer around pigment particles with high molar mass dispersant.

Effect of solid content on viscosity, between 0% to 8%, was examined at UV waterless offset inks. As solid content inside the ink formulation was increased, higher viscosity values were measured. All samples showed a shear thinning behavior but the degree of shear thinning behavior became more obvious with higher pigment contents. The increase in pigment content increased the density of the network structure so does the viscosity (Jia et al., 2011).

The effect of solid content in the 15% to 25% range on viscosity of inks was investigated in another research paper. The results of this study have shown that the viscosity of ink increased with solid content. In this study, surface area, fineness, effect of yttrium stabilized zirconia was examined with pigment surface areas of 12.3, 6.2 and 3.1 m^2/g. The inks with finest powder with the highest surface area showed higher viscosities than others. The higher surface area increased interparticle interaction between powders and this led to viscosity increase (Mücke et al., 2014).

Interaction between acrylic resin and carbon black particles with different particle morphologies was rheologically investigated. Dispersions were prepared with fixed particle volume fraction $\phi_{particle} = 0.15$ and different polymer volume fractions of $\phi_{polymer} = 0.053$, 0.11, and 0.21. Dispersions showed a Newtonian behavior at low shear stresses and behaved shear thinning above a critical stress value. Fractal particles had higher viscosities at low shear stresses than spherical particles and particle morphology effect

became negligible at high shear stresses. Polymer volume fraction of 0.053 was found suitable to stabilize particles in dispersion. Non-adsorbed polymer was present in dispersion at polymer concentrations higher than 0.053. Higher polymer volume fractions increased low shear stress viscosity due to the formation of a network structure between particles by excess amounts of polymer. Rheology of polymer solutions without carbon black particles was investigated for the determination of the solution viscosity shear stress graph. Solutions prepared with different concentrations of polymer showed a Newtonian like behavior and viscosity was increased with polymer concentration due to the formation of a network between polymer chains. The role of the interaction between adsorbed polymer layer and polymer in continuous phase was investigated by measuring diluted rheology of dispersions with constant $\phi_{particle}$ to $\phi_{polymer}$ ratios. Dilution viscosity was decreased significantly and intermediate Newtonian behavior between low and high shear stresses was lost especially at very low particle volume concentrations. Viscosity at low shear stresses decreased pronouncedly for spherical particle containing dispersions (Barrie et al., 2004).

Particle size and particle size distribution plays an important role on rheology of dispersion. Monomodal dispersed hard spheres can be packed in several ways: Cubic, body centered, tetragonal, face centered cubic and hexagonal close packing. It has been suggested that face centered cubic and hexagonal close packing has the maximum packing factor of 0.74. In monomodal systems, dispersions with small sized particles are more viscous than dispersions containing larger sized particles.

Viscosity of bi-modal (broad size distribution) dispersions is lower compared to monomodal size distributed dispersions. This behavior is related to filling the voids between large particles with small ones. The investigation of the effect of bimodal dispersions of sterically stabilized particles on rheology has been investigated extensively by researchers.

Fumed silica (FS) with 0.07μm particle size and silica powders with P10 (coarse), P500(intermediate), P600 (fine) having mean particle sizes of 19, 6.5 and 2.2 μm were used to investigate milling time, size ratio and FS ratio on rheological behavior. Suspensions were prepared with coarse particles (P10) and FS showed a shear thinning behavior. Extend of shear thinning behavior was increased with addition of FS and decreased with grinding time. On the other hand, suspension of finer sand powder (P600)

showed shear thickening behavior and this behavior was increased with fumed silica addition and decreased with grinding. Intermediate sized sand particle containing suspension showed shear thickening behavior with 5 wt% FS addition and this behavior was changed with addition of 15wt% FS to shear thinning behavior. Viscosity of ground suspensions was lower than those prepared by simple mixing. This showed less resistance to flow and packing fraction was improved. Grinding decreased particle sizes of coarse powders and de-agglomerated FS particles. The viscosity was decreased when packing ability of particles increased (Olhero & Ferreira, 2004).

Rheological behavior of ceramic inks prepared by nano-sized $CoAl_2O_4$ in water-based system was investigated. Na-Octanoate and polyacrylic acid with Na+ salts (Na-PAA) dispersants were used with ratios of 0 to 2.0 mg/m^2 by dispersant to the surface area of the ceramic pigment. All samples had a shear thinning behavior regardless of the dispersant type/ratio, but the viscosity of the inks prepared with Na-PAA decreased much compared to samples with Na-Octanoate. This behavior could be explained by an effective adsorption of Na-PAA on pigment particles and the formation of repulsive forces between pigment particles. Investigation of the stability of samples with both dispersants were conducted by sedimentation analysis for two months and less sedimentation was observed for samples prepared with Na-PAA. This also shows formation of repulsive forces and prevention of flocculation by adsorption of Na-PAA on pigment particles (N'gouamba et al., 2020).

3.1.2. Yield Point

Many fluids do not flow with shearing stress application instantly. They start to flow only after a critical stress. This critical stress is called as yield point and shows the strength of the particle network in dispersions. Yield point arises from interparticle interactions or networks generated by Wan der Walls forces, hydrogen bonds or electrostatic forces. Interparticle network of dispersions generates forces that restrict deformation by externally applied force. If externally applied forces are lower than internal network forces, dispersion behaves elastically, and only small deformation occurs. When external forces are higher than internal forces, internal structure collapses

and flow starts. Elastic behavior changes to viscous behavior at flow condition. Generally, yield stress of dispersion increases with higher viscosity due to particle interactions.

3.1.3. Thixotropy

Most of the pigmented inks such as offset, gravure etc. show thixotropic behavior. Thixotropy is a phenomenon in which the microstructure of a fluid is broken down under shear and returns to initial condition at rest. Figure 3.6 demonstrates 3D breakdown and built-up of suspension structure with thixotropic behavior. In thixotropic materials, the viscosity decreases with shear rate increase. The ink structure restores time-dependently to the initial viscosity value approximately when no more shear stress is applied.

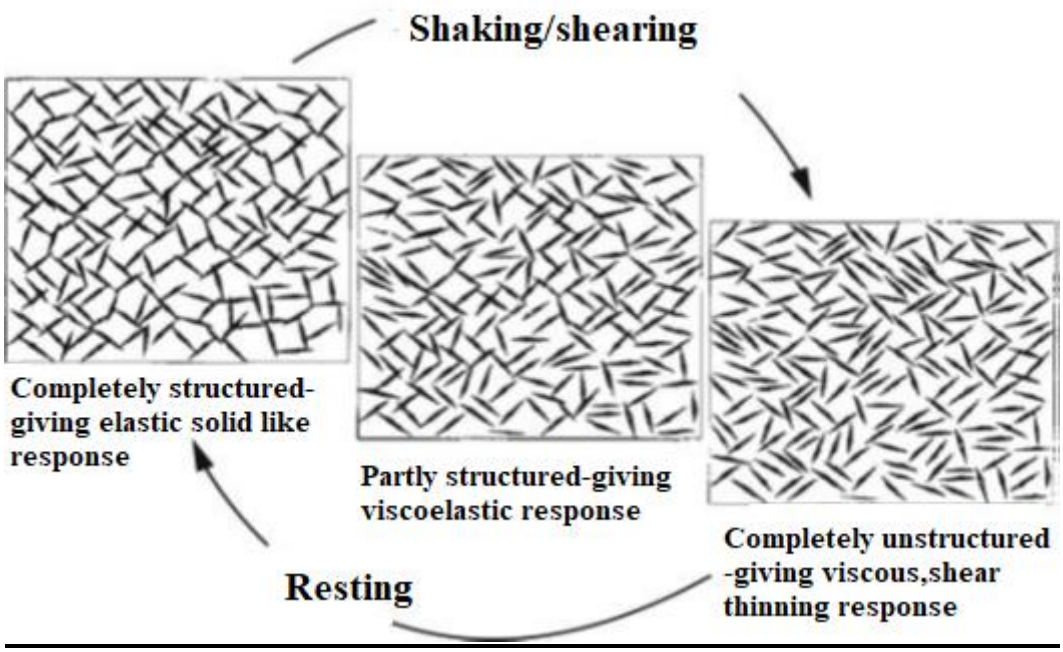

Figure 3.6. Break-down of thixotropic structure

(Source: Barnes, 1997)

The rheological behavior of thixotropic materials can be understood by microstructure changes and directly related to weak attractive forces between particles. Formation of particle aggregates results in space-filling particle network. These space

filling networks are weak to resist stresses revealed during flow. Flocs are separated from each other and flow. In case of low shear forces or resting network between particles rebuilds (Mewis & Wagner, 2009).

Thixotropic fluids show specific hysteresis curves depicting the time effect of restoring to the initial viscosity. In loop test, thixotropy is measured by determining area between hysteresis loops which form by ascending and descending loop of viscosity shear rate curve. Figure 3.7 shows thixotropy in graphical form. Flow curve I, upward curve, shows behavior with shear rate increase and flow curve II, downward curve, shows behavior while gradually lowering shear rate. Area between upward and downward curves is called as hysteresis area and its size is a measure of the degree of thixotropy. Upward and downward curves of dispersions without thixotropy overlap over each other and that means zero hysteresis and no thixotropic behavior.

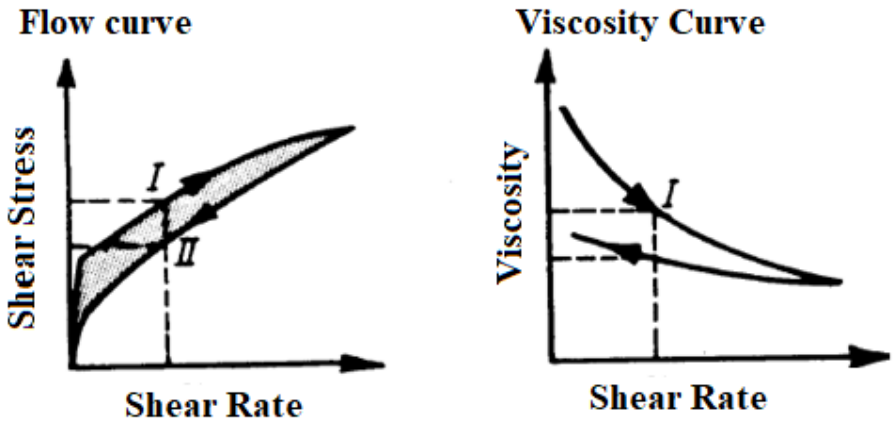

Figure 3.7. Thixotropy diagrams

(Source: Schramm, 1998)

Rheology of screen-printing inks were investigated for fabrication of porous nickel (NiO) and scandia-stabilized zirconia (ScSZ) anodes. Samples of A and B prepared by Terpineol and Texanol solvents respectively and Ethyl cellulose was used as binder for both samples between the range of 0 wt% - 5 wt%. Inks with lower solid content showed non-thixotropic behavior. Poor thixotropic behavior of inks was directly related with poor pigment dispersion and poor particle network. Samples prepared without binder

(26 vol% solid and 0 wt% binder) showed poor thixotropic behavior. Thixotropy and viscosity of both Terpineol based NiO/ScSZ (26 vol% solid) and texanol based NiO/ScSZ (26 vol% solid) inks were increased as binder content increased (Somalu et al., 2011).

3.2 Dynamic Properties of Inks

Viscosity measurement is not sufficient to explain rheological properties alone and viscoelastic behavior must be understood. The use of dynamic measurements for the examination of the ink microstructure and network properties is more reliable.

3.2.1. Elastic (G') and Viscous (G'') Modulus

Microstructure of structural liquids has minimum energy during rest condition. Forces start to restore rest condition when a deformation is applied to structural liquids. Applied deformation initiates microstructural changes and viscous forces start to dissipate. Elastic forces arise from resisting microstructural forces to externally applied forces. These viscous and elastic forces produce viscoelastic effects. Materials that show both elastic and viscous behavior simultaneously are called as viscoelastic.

There are various tests for the measurement of viscoelastic response which are mainly categorized as creep test, oscillatory test, stress relaxation test and start up test. Oscillatory test is one of the most frequently used tests for the characterization of the viscoelastic response of dispersions. A sinusoidal stress or strain as a function of frequency (w) is applied to samples and resulting output is evaluated. Sinusoidal stress or strain output to applied in-phase sinusoidal input represents solid-like behavior. Out of phase response to input corresponds to liquid like behavior. Solid like and liquid like behaviors are characterized by storage modulus (G') and loss modulus (G'') respectively. These parameters are dependent on frequency applied, ω, which is given by $2\pi f$, where f is the frequency in hertz (Hz). When an oscillatory shear strain is applied to a viscoelastic material as a function of frequency ω and amplitude of γ_o, material will respond with a sinusoidal shear stress (τ) with amplitude of τ_0 and phase will shift by an angle δ. Sin waves of strain input and stress response are shown in Figure 3.8. Applied strain and resultant stress are depicted as:

$$\gamma(t) = \gamma_o \sin \omega t \quad (3.4)$$

$$\tau(t) = \tau_0 \sin(\omega t + \delta) \quad (3.5)$$

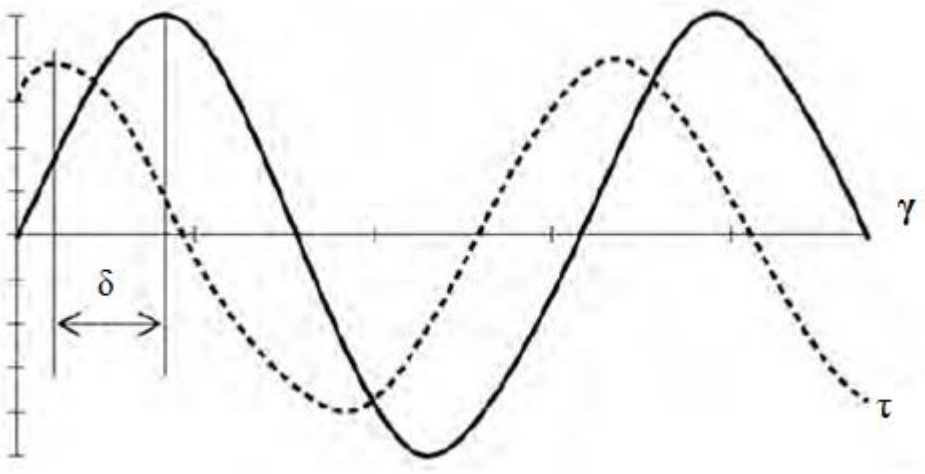

Figure 3. 8. Viscoelastic behavior: Time dependent behavior of oscillating strain and the stress

(Source: Mezger, 2014)

Phase shift angle δ range between 0° and 90°. Phase shift disappears for elastic materials and δ is 0° while phase shift is 90° for viscous materials. In oscillatory measurements, resistance to deformation is written in complex modulus form which is expressed as:

$$G^*(w) = \tau_0 / \gamma_0 \quad (3.6)$$

Complex modulus consists of elastic modulus G' and viscous modulus G'' which represent in-phase and out-phase components with applied strain. G' and G'' are defined as:

$$G^*(w) = G'(w) + iG''(w) \quad (3.7)$$

$$G'(w) = G^*(w) \cos(\delta) \quad (3.8)$$

$$G''(w) = G^*(w) \sin(\delta) \quad (3.9)$$

Dynamic properties of inks are more important than steady state properties in the explanation of particle network structure. Viscoelastic properties of inks are defined by elastic G′ and viscous G" modulus. Elastic G′ modulus is defined as the measure of elasticity of material which means ability of energy storage, while G" describes the viscous dissipation of energy which provides viscous resistance. Amplitude and frequency sweep tests are necessary for the determination viscoelastic properties.

3.2.2. Amplitude Sweep

Amplitude sweep tests are performed at various amplitudes at constant frequency. Depending on application of strain or stress, test is called as strain sweep or stress sweep respectively. Mostly strain sweep tests are used in fundamental structure related research. Strain sweep test will be described in more detail due to the above reason. Strain sweep measurements are conducted by keeping frequency ω constant and G *, G ′ and G'' are measured as a function of strain. A typical strain sweep graph is shown in Figure 3.9 below.

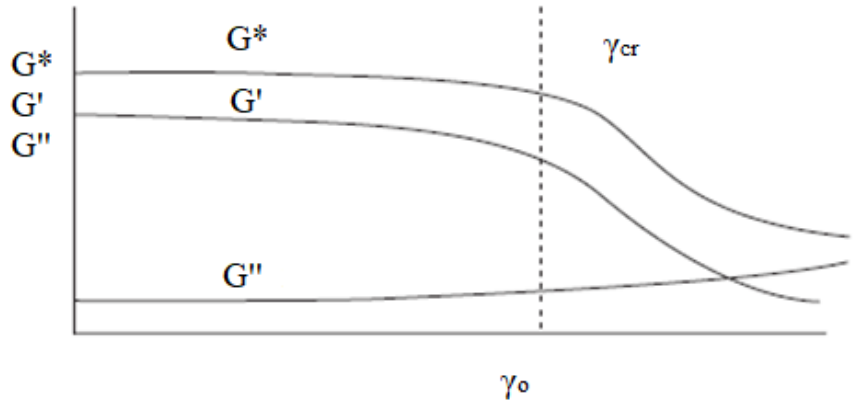

Figure 3.9. Strain sweep diagram

(Source: Tadros, 2010)

G', G'' and G* values remain constant until γ_{cr} and this constant plateau is called as Linear Viscoelastic Region (LVER) as shown in Figure 3.9. Amplitude sweep tests are performed only to determine limits of LVER. After γ_{cr}, G* and G' value decrease

while G'' value increases in the non-linear region. Before γ_{cr} structure keeps its order and after γ_{cr} structural deformation starts irreversibly. Viscoelastic characterization of materials can be conducted by evaluating the length of LVER. Elastic behavior dominates if G' > G'' and viscous behavior dominates if G''> G' in LVER. The dynamic test should start with a stress or strain amplitude test towards the determination of the LVER. Sometimes elastic modulus G' and viscous modulus G'' are in balance and that point is called as gel point. Generally, G' is used for determination of LVER due to the tendency to leave LVER and deviation is higher than G'' in experiments.

Rheological properties of silver pastes with 4 commercial products were investigated by Thibert et al. (2014). Samples A and B were prepared with same vehicle (2-(2-butoxyethoxy) ethanol and rosin), sample C contained same solvent but another binder while sample D was prepared with a totally different vehicle. All samples showed shear thinning behavior and the main difference between samples was their yield stress values. Sample A had the largest yield stress value, followed by B, D and C samples respectively. Due to complex shear history of pastes during screen printing, an oscillatory measurement was performed. Different shear stress values were selected to perform oscillatory tests representing the three steps of screen printing based on stress sweep tests. Stress selected for pre-print and post-print steps was τ_0=10 Pa (in the LVER) while τ_0=3000 Pa was selected for the simulation of print step. All pastes had solid-like behavior and loss tangent was 15 ° in pre-print and post-print stages. When stress reached to 3000 Pa they became liquid.

3.2.3. Frequency Sweep

Frequency sweeps are oscillatory tests that are performed at various frequencies at constant amplitudes. Before performing a frequency sweep test for any sample, LVER must be determined by strain or stress sweep test. Figure 3.10 shows viscoelastic behavior determined by frequency in LVER. Frequencies represent inverse of time scale. Larger the frequency shorter the time scale and shorter the frequency larger the time scale.

Relationship between dispersion stage and rheological properties were investigated. Dispersion stages were provided by dispersant amounts for three different ink-jet inks. Sample without dispersant was called as normal dispersion. The other two dispersions were prepared by 2 wt% and 10 wt% dispersant respectively. For normal

dispersion G′ was higher than G" at low frequencies which indicates predominant elastic response. G" became higher than G′ at higher frequencies. Results showed normal dispersion exhibited both elastic and viscous response. For 2% dispersant added ink, G" was higher than G′ at all frequencies. These results showed relatively weak attraction between pigment particles which indicates a stable dispersion. In the case of 10 % dispersant added ink G′ is higher than G" which was indicative of highly attractive forces and flocculation. Ink printability was also investigated by inks at different stability levels. Landing position of each ink drop was compared with determined target position. Positioning accuracy was increased as the level of stability increased (Woo et al., 2013).

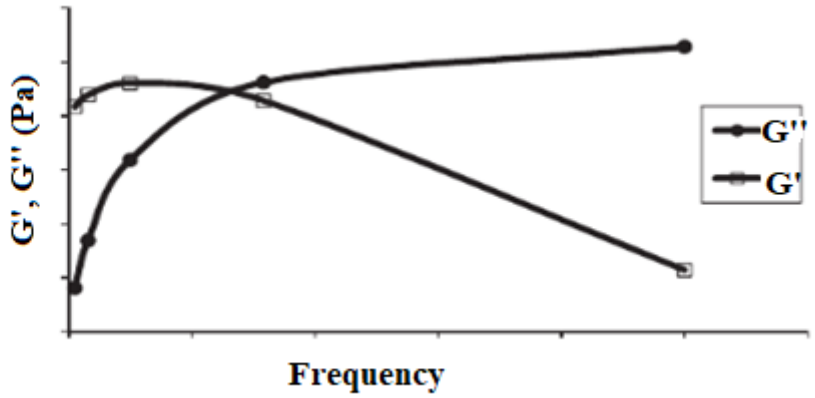

Figure 3.10. Frequency sweep test

(Source: Norton et al., 2011)

3.2.4. Loss Tangent

Loss tangent describes ratio of the two parts of the viscoelastic behavior. Loss tangent shows the relationship between energy loss and energy stored. It is calculated as the ratio of G'' to G' as shown in Eqn.3.10. For fully elastic behavior ($\delta = 0$) there is no viscous portion. For ideally viscous behavior ($\delta = 90°$) there is no elastic portion. Balance between viscous and elastic modulus occurs at $\delta = 45°$. $\tan\delta = 1$ represents transition from liquid to solid state and loss tangent values below and above that point can be summarized as shown below:

$$\text{Tan } \delta = G''/G' \qquad (3.10)$$

$\text{Tan } \delta > 1$ (since $G'' > G'$) Liquid behavior dominates

$\text{Tan } \delta < 1$ (since $G' > G''$) Solid behavior dominates

$\text{Tan } \delta = 1$ (since $G' = G''$) Critical point

Stability assessment of some cosmetic systems was determined by oscillatory shear measurements. Rheological oscillatory tests were used to quantify internal structure and rigidity of viscoelastic systems. Limiting value of LVER showed maximum tolerated deformation by sample. Cream containing crosslinked acrylic polymer had the longest LVER due to strong intermolecular associations. This structure also provided higher stability to cream. On the other hand, xantam gum containing sample had lower LVER limiting value and structure was unstable. After determination of LVER, frequency sweep test applied to the samples have shown solid like behavior with G'>G'' over the entire frequency range. At low frequencies ($\omega \leq 0.1$ rad/s) G' value gave information about long term stability of system. All samples had G'>10 Pa which indicated stability of the system (Ibănescu et al., 2010).

Oscillatory stress sweep test was applied to investigate the viscoelastic behavior of lead-free solder pastes with nomenclature of DOE2, DOE4, DOE5, DOE8. The ratio of G''/G' was interpreted as an indication of strength of interaction between particles. DOE4 and DOE8 samples with the lowest value of G''/ G' was interpreted as tacky and cohesive which will have poor paste release during printing. Cross over stresses at G'=G'' was compared and DOE8 sample with highest cross-over point was selected tackier and more cohesive because paste will require more stress to pass from solid to liquid behavior. Phase angle within the whole stress range were examined and phase angle of the DOE4 and DOE8 samples fluctuated while phase angle of DOE5 and DOE8 were increasing with stress. This fluctuation of phase angle was interpreted as sedimentation of metal particles, and phase separation between particles from vehicle was observed for these samples (Durairaj et al., 2009).

Suspensions that were prepared by blue shade benzimidazolone pigment (R 176) with volumetric ratios of ϕ = 0.005, 0.027, 0.056, 0.087, 0.119, 0.154, 0.191, 0.23, and 0.272 showed higher shear thinning behavior with pigment content increase. Liquid-like behavior was dominant over solid like behavior and negligible dependence on strain was observed at volumetric ratio of ϕ b =0.119. G' value becomes higher than G'' value at a higher volumetric ratio than ϕ=0.154 (Salamon et al., 2020).

Rheological properties of nanoparticle agglomerates in the form of network structure were studied and hydrogen bonds were found to be the key parameter on fumed nano silica agglomerate formation and rheology. Effects of solvents (terpinol and BCA), content of binders, and surface properties of fillers (surface untreated SiO_2, surface treated SiO_2 with silane and dielectric powders) on rheological properties were investigated. All prepared pastes (inks) showed shear thinning behavior. Pastes with surface untreated SiO_2 had the highest viscosity because of extensive friction between binder and filler. There was less friction between binder and filler due to silane's lyophilic and lyophobic groups. The viscosity was found lower for surface treated SiO_2 containing dispersions. On the other hand, BCA solvent containing inks showed higher viscosities than terpinol containing inks. Poor wetting and higher viscosities were a result of higher hydrophobicity of BCA than terpinol due to hydroxyl groups of SiO_2. Different polarities of solvents had effects on thixotropic and viscoelastic properties. According to dynamic experiment results, loss tangent decreased with binder content increase. G' and G'' of BCA containing ink showed an intersection point at 6 wt% binder content. This point was interpreted as entanglement point and the reason for higher viscosities. Increase of binder content to 10 wt%, resulted in agglomeration and dropped G' to lower values than G' of 6 wt% binder content inks (Lin et al., 2008).

Polydispersity effect on suspension viscosity and elastic modulus was studied with aqueous dispersion of polystyrene latex. Three different suspensions were prepared at narrow, moderately broad and broad particle size distributions. Suspensions with different particle size distributions showed shear thinning behavior. Increase of particle size volume fraction increased rate of viscosity decrease. At low volume fractions of all latex suspensions, G'' was bigger than G' due to the absence of interparticle interactions. G' became higher than G'' due to repulsive interactions of particles with increasing volume fractions of particles. Viscosity reduction was observed with increase of particle size distribution. Yield value of suspensions were decreased with increasing particle size distribution because small particles could fit between larger particles to minimize particle interactions. Similar reasoning was also stated for increasing extent of shear thinning behavior (Luckham & Ukeje, 1999)

CHAPTER 4

COLOR STRENGTH

Color results from the interaction between light, object, and observer. Light is formed by waves and each wave has a wavelength. Human eyes have light sensors which are sensitive to visible spectrum with wavelengths of 400 nm to 700 nm.

Surfaces reflecting most of the visible light in all directions (diffuse way) appear to human eye as white. Objects or printed surfaces that absorb all light are perceived as black. Objects absorbing only some part of light spectrum appear as colored and observed color is also related with wavelength to the reflected light.

When light strikes a surface, transmission, reflection, scattering, absorption, or transmission can occur and this is shown in Figure 4.1. Passage of light through a material without any change is called as transmittance. During reflection, a small amount of light penetrates paper and bends. This is called refraction and finally is scattered by ink or printed surface. Absorption is transformation of light energy to another type of energy which is generally heat. When light strikes to a surface some part of light is absorbed while the remaining part travels in many directions or scatters.

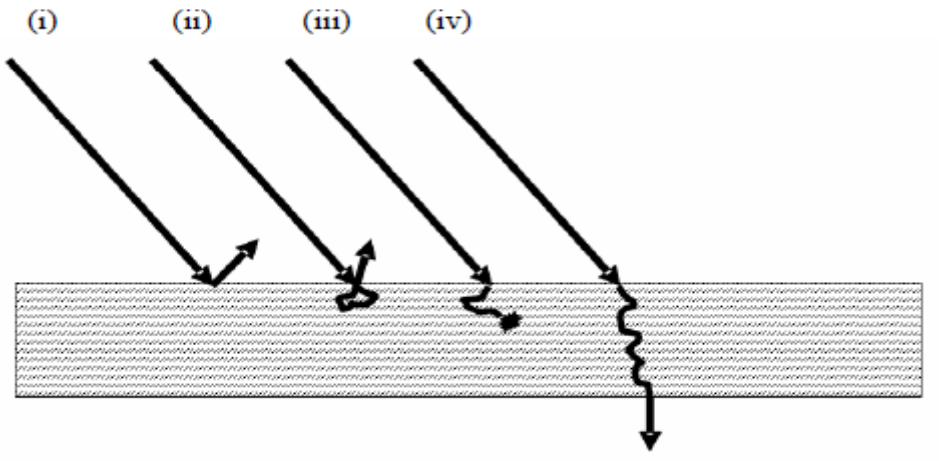

Figure 4.1. Interaction of light and surface optically

(i)light reflected at the surface,(ii) light scattered by the paper structure,(iii) light absorbed by paper or printed ink and (iv)light transmitted through the paper.

(Source: Andersson & Norberg, 2007)

When light strikes to a printing surface, some light is absorbed or scattered from surface. Remaining part of light could be reflected by printing surface or ink. The purpose of ink on the surface is to absorb some specific wavelengths of light and reflect other non-absorbed wavelengths from surface. Light wavelengths left from surface are changed and reveal a new color and wavelength pattern forms surface's spectral data, which is also its fingerprint.

Color measurements can be made in a variety of ways, but the use of spectrophotometers is the most common quality control method. The main components of spectrophotometers can be listed as: illumination, specimen for reflection or transmittance, dispersing light equipment, detector, and signal analysis system. Light of illumination strikes to a dispersing light equipment which works like a prism and light separates to different wavelengths. Only one wavelength reaches to surface and interacts with surface afterwards. Detector part measures transmittance and absorption with mathematical calculations.

Color strength or tinting strength of an ink is imparting color ability to system. During printing, color observed on print surface is a result of optical properties of pigment. Strength of color is generally determined by comparing with another standard or reference. Color strength of an ink is directly related with particle size distribution, film thickness on applied surface and pigment content of ink. Well dispersed pigment ink provides higher color strength.

Different grinding conditions were investigated for water-based color pigment slurry. Milling was performed at 80 % filling of grinding chamber volume and constant flow rate of 50 $L.h^{-1}$. Depending on grinding process, specific energy and stress intensity of grinding medium was calculated with formulations of Eqns. 3.11 and 3.12 respectively. Bead sizes were changed between 0.4 mm - 0.5 mm and 1 mm- 1.2 mm having different bead densities. Apart from bead properties, stirrer rotation effect was determined at 8 m s^{-1} and 12 m s^{-1}. Best milling efficiency was achieved by adjusting bead size, density of beads and stirrer rotation speed.

$$Em=(N-No)/m \qquad (3.11)$$

$$SIgm=d^3pVt^2 \qquad (3.12)$$

Some terms used in Eqn. 3.11 and Eqn. 3.12 are: E_m was specific energy value added to dispersion, N_o was the energy that was required to rotate un-filled mill and N was energy necessary to rotate mill with bead loading. SI_{gm} showed energy intensity of grinding medium and d, p and V_T are bead size, bead density and stirrer angular speed respectively. Relationship between particle size and specific energy was investigated and best particle size with lowest specific energy was achieved with condition of smallest bead size (0.4-0.5 mm), highest bead density and lower tip speed of 8 ms^{-1}. This milling condition also provided the highest color strength. Apart from grinding condition, milling time increase changed color of red dispersion from bright red to dark red and "L" value decreased to lower values which showed higher color strength and lower particle size. It was found that brightness "L" value was directly proportional to particle size. Minimum energy requirement to reach mean particle size DV_{50}=0.55 µm was also achieved by smaller bead size 0.4 mm- 0.5 mm with lower rotation speed of 8 ms^{-1} (Weber, 2010).

Dispersed and well-spaced pigment particles in medium provide higher color strength. Influence of surfactants with different Hydrophilic Lipophilic Balance (HLB) on dispersibility of Yellow 110 pigment in aqueous medium was analyzed. Surfactant of Secondary Alcohol Ethoxylate with 13.3 HLB provided the best consistency in terms of color strength at different concentrations and color strength was measured between 98 and 101 while others had deviations in strength (Nagose & Rose, 2019).

Color strength of a dispersion depends on particle size, particle shape and state of dispersion. Color strength increases with decreasing particle size because pigment particles start to cover larger areas on printed surface. During gravure and flexographic printing process color failure can occur and reasons for these failures were investigated in 5-7 hours duration. Pigment particle size was decreased and the highest decrease from 482 nm to 232 nm was observed at black base during printing. The decrease in particle size during printing improved gloss and color strength (Frimova et al., 2005).

Chitin and chitosan were used as dispersant to investigate effect on quinacridone red pigment and compared with cellulose. SEM images showed that cellulose and chitosan prevented agglomeration of quinacridone red pigments while chitin had lower effect on agglomeration. Lightness and redness values increased with the use of chitosan and cellulose (Saito et al., 2020).

CHAPTER 5

EXPERIMENTAL STUDY

This chapter introduces the materials, dispersion preparation, rheology, particle size measurement and color strength measurement steps. Concentrated dispersions of carbon black pigments in solvent-borne medium were prepared in the first stage of the work. Rheological measurements were conducted, and the inks were printed on paper for the investigation of the effect of rheology on printing performance afterwards.

5.1. Materials

Carbon black was used for dispersion preparation was obtained from Orion Engineered Carbons. This pigment was characterized by an average particle size of 31 nm and BET (surface area) of 62 m^2/g according to the information supplied from the manufacturer. Pigment content of dispersions varied between 20 wt% and 30 wt%. A polymeric dispersant was used to investigate the effect on dispersion state and changed between 0 wt% to 0.75 wt%. Commercially available nitrocellulose (NC) resin containing varnishes were used due to the combustible nature of NC resins. Ethoxy Propanol, also known as propylene glycol ether, was used as solvent in dispersions.

Carbon black pigment, dispersant, solvent, and varnish were coded as P, D, S and V respectively. The numbers at the beginning of codes showed weight ratios present in dispersions.

Glass beads with sizes of 1.3 mm were used for regular dispersions. Only grinding medium effect investigated dispersions were ground with 0.5 mm and 0.8 mm yttrium stabilized zirconia beads. Bulk densities of 0.5 mm and 0.8 mm beads were 3.73 kg/dm^3 and 3.66 kg/dm^3 and were obtained from Netzsch Group.

5.2. Dispersion (Ink) Preparation

Dispersions were prepared by using a high-speed mixer and dispersion cup. Dispersion process was divided into three main parts which were pre-mixing, milling and let-down. High speed mixer was used for both premixing and milling stages. Predetermined amounts of varnish, solvent, carbon black, was weighted in the dispersion cup initially. In pre-mixing stage, carbon black, solvent and varnish were mixed at 5100 Rpm without beads for 30 minutes. The purpose of the pre-mixing stage was effective wetting of pigment particles and same ratios were used for all samples to prevent deviations due to wetting stage. Beads were added to the dispersion cup and dispersions were ground during 30 minutes with 5100 Rpm after premixing. Weight ratio of bead to carbon black mixture was 2:1 for obtaining effective dispersion.. At let-down process, remaining parts of formulations were added to complete formulation to 100 wt%. During pre-mixing and milling stages some solvent was evaporated since there was no cooling jacket around the dispersion cup. This evaporated amount was added to samples at the end of let-down process. Dispersion and beads were separated by using 100 microns sieve after let-down process. Prepared dispersion (ink) samples are listed in Table 5.1 and a visual flow of ink preparation steps are shown in Figure. 5.1. Totally 19 different samples were prepared.

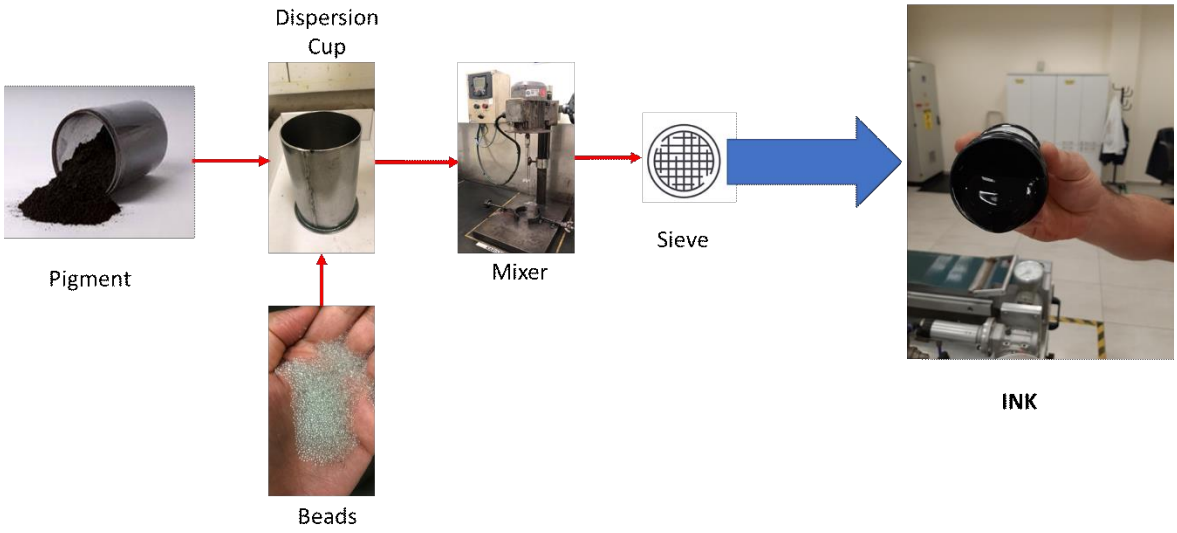

Figure 5.1. Visual flow of ink preparation steps.

5.3. Rheological Measurements

Rheological measurements were conducted with Haake Mars II Advanced Rheometer using the plate-plate sensor of PP35Ti. Rheological behavior of dispersions was determined by both steady shear and dynamic shear measurements. Measurements were done at 20 °C and gap size between plates was adjusted to 1 mm. Before dynamic shear measurements, pre-shearing wasn't applied, only samples were shaken in small jar, to prevent evaporation of solvent. Rheological methods are tabulated in Table 5.2.

Table 5.1. Prepared carbon black dispersions.

	P (% wt)	D (% wt)	V (% wt)	S (% wt)	Grinding Time (min)	Bead Size (mm)
Dispersant Effect	20	-	45	35	30	1,3
	20	0.25	45	34.75	30	1,3
	20	0.5	45	34.5	30	1,3
	20	0.75	45	34.25	30	1,3
Pigment content Effect	25	-	42	33	30	1,3
	27.5	-	41	31,5	30	1,3
	30	-	40	30	30	1,3
Varnish-Solvent Ratio	20	-	40	40	30	1,3
	20	-	45	35	30	1,3
	20	-	50	30	30	1,3
	20	-	55	25	30	1,3
Grinding Medium Effect	20	-	45	35	30	0,5
	20	-	45	35	30	0,8
Grinding Time Effect	25	-	42	33	30	1,3
	25	-	42	33	60	1,3
	20	-	45	35	30	1,3
	20	-	45	35	60	1,3
Storage Period Effect	20	-	45	35	30	1,3
	20	0,5	45	34,5	30	1,3

Table 5.2. Parameters used in rheological measurements

Rhelogical Method	Details
Viscosity	$\dot{\gamma}$ =0.01-100 1/s, (stepwise)
Thixotropy	**1.** $\dot{\gamma}$ =0.01-100 1/s **2.** $\dot{\gamma}$ =0 (60s) **3.** $\dot{\gamma}$ =100-0.01 1/s
Strain Sweep	τ=1-100 Pa, f=1 Hz γ =0.1-100, f=1 Hz
Frequency Sweep	f=0.1-10.0 Hz

5.4. Particle Size Measurement

Particle size measurements were performed with Malvern Mastersizer 3000 based on dynamic light scattering (DLS). Before starting measurement, 5 drops of ink were added to 10 ml of ethanol solvent and mixed. This operation was done for staying in the obscuration range of the particle size analyzer. Obscuration range was adjusted between % 4 and % 8 to prevent multiple scattering. After that, diluted sample was added to dispersion chamber and particle size measurements were conducted. Rotation speed was adjusted to 1600 rpm during the measurements.

5.5. Printing

Different ink dispersions were printed on papers with RK printing proofer which is shown in Figure 5.2. Size of fields was 14 x 16 mm and printed at speed of 1 ms^{-1}. Paper was attached to a rubber roller of RK Proofer. Inks were transferred from plate to paper directly by the motion of the roller.

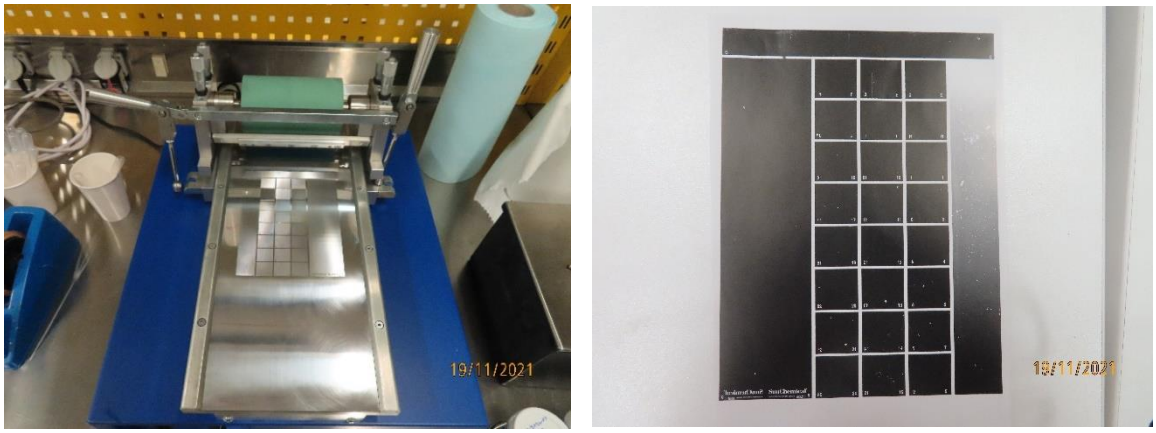

Figure 5.2. RK proofer and printed paper.

5.6. Color Strength Measurement

Figure 5.2 shows printed carbon black dispersion with RK Proofer. Color strength of printed samples was realized with Datacolor TM 400 spectrophotometer. Measurements were done from 3 different points on the printed surface, left, right and middle, and average of these measurements was reported. Color strength measurements were performed with settings of D 50 illuminant and density filter was 2 degrees. Color strength comparisons were made according to reference sample which assumed color strength of 100 %. Reference samples were selected randomly for all investigation parts and results higher than 100 % (according to reference) showed stronger color strength property.

CHAPTER 6

RESULTS AND DISCUSSION

6.1. Dispersant Content Effect on Rheological Properties of Carbon Black Inks

6.1.1. Dispersant Effect on Viscosity

The rheological behavior of dispersions with various dispersant ratios was investigated. Concentration of the dispersant varied from 0 to 0.75 % by weight. Viscosity flow curves of dispersions are given in Figure 6.1. Dispersion prepared without dispersant showed shear thickening behavior and viscosity increased from 0.75 Pa.s to 13 Pa.s at shear rates between 0.01 s^{-1} and 0.18 s^{-1} . After reaching maximum viscosity of 13 Pa.s, dispersant free dispersion exhibited shear thinning behavior from 13 Pa.s to 1.42 Pa.s between 0.18 s^{-1} to 100 s^{-1}. Dispersant containing dispersions had lower viscosity than the dispersion without dispersant over the entire range. This behavior can be explained by the adsorption of the dispersant on the pigment particles which prevented agglomeration. Dispersant content increase within the range of 0.25 wt% to 0.75 wt%, resulted in higher viscosities between 0.01 s^{-1} and 100 s^{-1} range. The viscosity increased as the proportion of dispersant increased, which may be due to the contribution of excess dispersant to excess structure formation. Some abnormality was observed while measuring the viscosity of the sample containing 0.25 wt % dispersant at 0.36 s^{-1} strain and some sedimentation was determined for that dispersion. This may account for the lower viscosity of 0.25 wt% dispersant containing sample. No sedimentation was observed in the other samples.

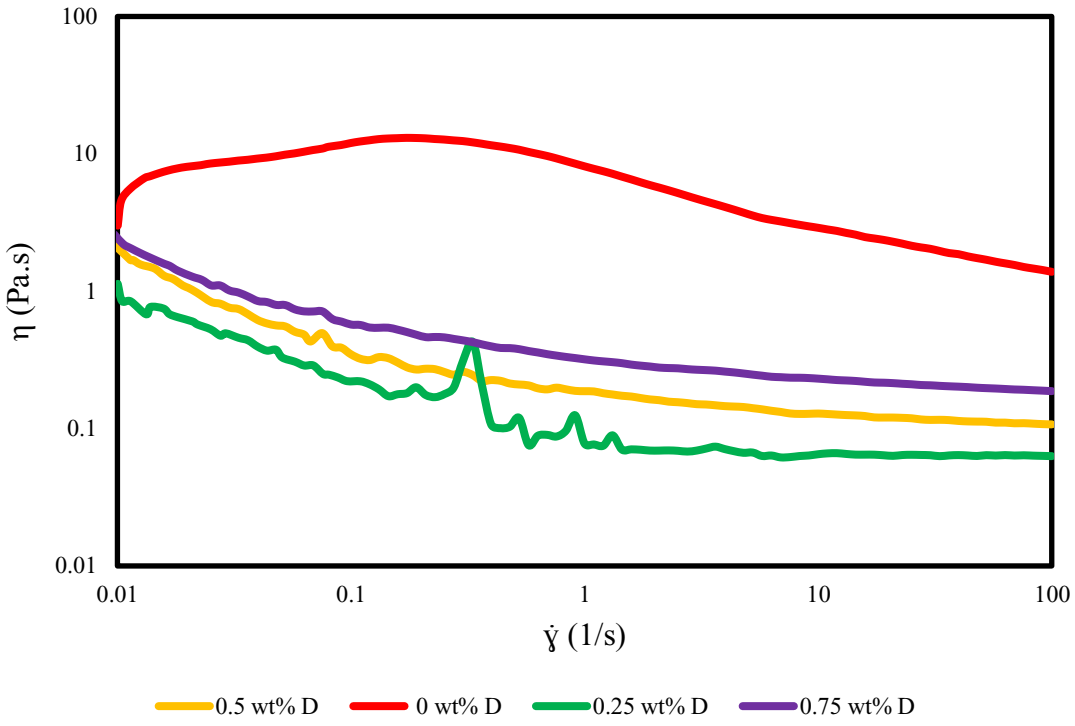

Figure 6. 1.Viscosity- shear rate graph of dispersions prepared with 0 wt%, 0.25 wt%, 0.5 wt %, 0.75 wt% dispersant.

6.1.2. Dispersant Effect on Dynamic Shear Rheology of Carbon Black Dispersions

Oscillatory measurements were performed to determine dispersant effect on viscoelastic properties and are given in Figure 6.2. Stress sweep test was used to determine the LVER at constant frequency of 1 Hz. G'' was dominant over G' all over the range for all samples. At low stresses, G' and G'' were parallel to stress axis and this plateau showed LVER. Dispersion prepared without dispersant had the lowest LVER, both G' and G'' rapidly decreased with stress increase. G' of dispersant free dispersion especially decreased from 24 Pa to 1.27 Pa in stress range of 1 Pa to 100 Pa. Main reason behind that behavior could be the breakdown of agglomerates with hydrodynamic forces.

Dispersant containing samples had less stress dependent behavior and higher LVER. This indicates dispersant formed an interparticle network, which showed minimum agglomeration. Dispersion prepared with 0.25 wt% dispersant had the lowest

G’ over entire range and some sedimentation was detected with the help of a spatula for that dispersion. Any sedimentation was not observed for other dispersions.

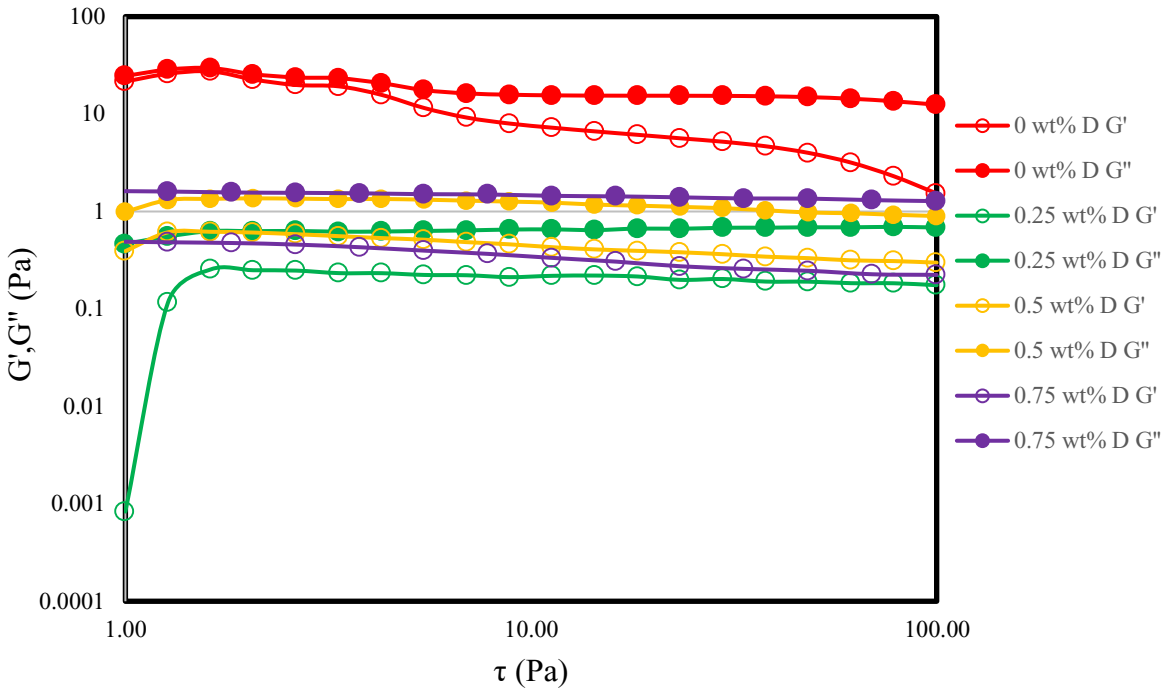

Figure 6.2. Stress sweep graph of dispersions prepared with 0 wt%, 0.25 wt%, 0.5 wt %, 0.75 wt% dispersant ratios.

Frequency sweep test was performed to investigate viscoelastic behavior of the dispersion in the linear range where the network structure was not deformed. Figure 6.3 shows frequency dependent storage and loss modulus in LVER at constant stress amplitude of 2 Pa for all samples. It was observed that both G’ and G’’ decreased with frequency decrease. All samples had higher G’’ than G’ which showed dominant fluid-like behavior.

Lower frequency values represent longer time periods. Loss tangent of dispersions prepared with 0 wt%, 0.25 wt%, 0.5 wt% and 0.75 wt% dispersant was found 6.01, 82.27, 7.42 and 58.96 respectively at 0.1 Hz. This showed dispersant free dispersion had more solid like behavior and gel-like response. This gel like structure can be attributed to the agglomerated structure of the dispersion due to absence of dispersant.

Sedimentation was observed for dispersion containing 0.25 wt% dispersant which also had lowest G' and the highest loss tangent value of 0.004 Pa.s and 82.27 at 0.1 Hz respectively. This lowest G' at low frequency range also showed instability of dispersion in long term.

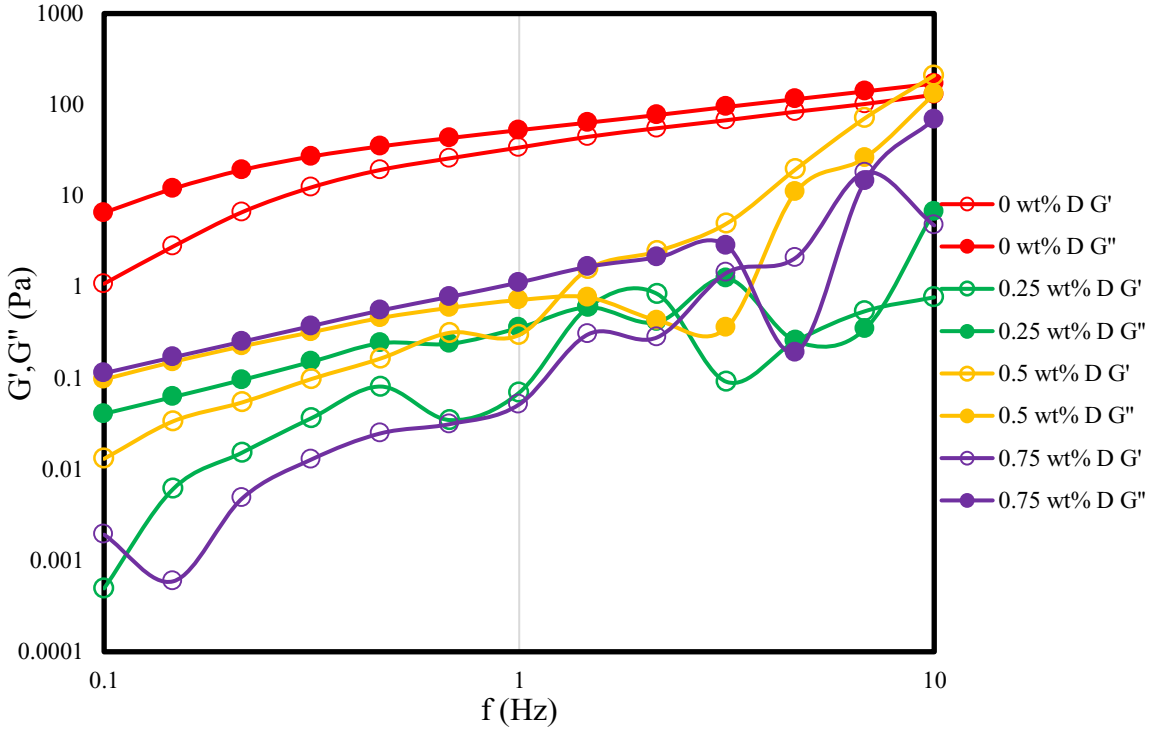

Figure 6.3. Frequency sweep graph of dispersions prepared with 0 wt%, 0.25 wt%, 0.5 wt %, 0.75 wt% dispersant ratios.

6.1.3. Dispersant Effect on Thixotropy

Thixotropic area of dispersions prepared at various dispersant contents are shown in Figure 6.4. Sample prepared without dispersant had the highest thixotropy while dispersant containing samples had lower degree of thixotropic behavior. As the dispersant content increased from 0.25 wt%, 0.5 wt% to 0.75 wt% thixotropy of dispersions also increased to 98, 142 and 219 $Pa.s^{-1}$ respectively. Thixotropic behavior of binder free dispersion was about 12 times higher than 0.5 wt% dispersant containing dispersion. Shearing of dispersant free dispersion disrupted aggregated structure and when shear was

removed, particles began to aggregate again, and structure wasn't recovered immediately. Shear induced break-down of flocs may require some time to recover resulting in highest thixotropic behavior of the dispersant free dispersion.

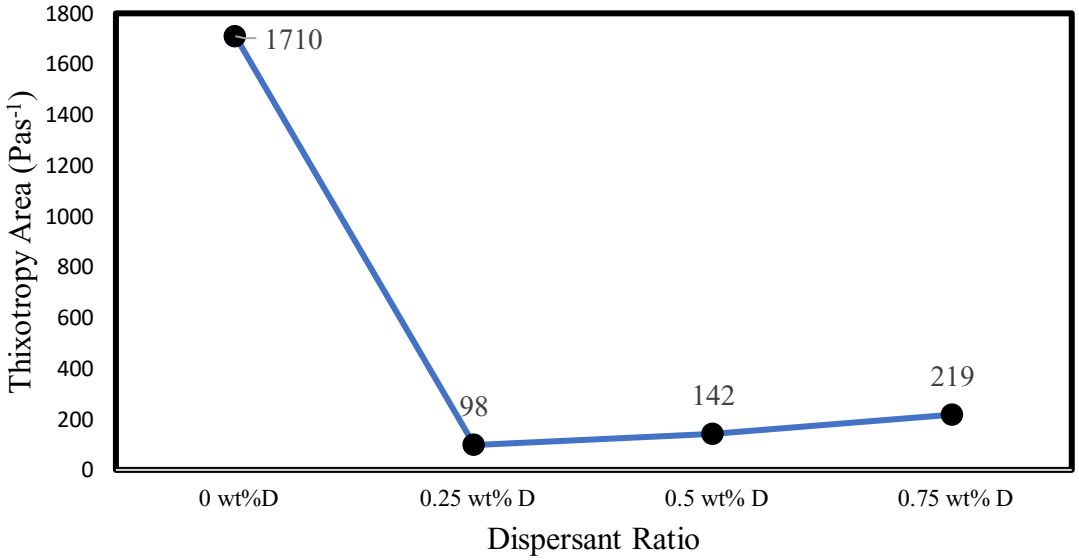

Figure 6.4. Hysteresis Loop Area (Thixotropy) comparison of dispersions prepared with 0 wt%, 0.25 wt%, 0.5 wt %, 0.75 wt% dispersant.

6.1.4. Rheology Effect on Color Strength for Dispersant Containing Carbon Black Dispersions

Color strength and loss tangents of dispersions with different dispersant contents are compared in Figure 6.5. Dispersion prepared with 0.5 wt% dispersant was selected as "reference sample" with color strength of 100 % and comparison of other dispersions were completed according to that reference. Color strength of 0 wt% and 0.75 wt% dispersant containing samples were measured as 97.62 % and 92.93 % accordingly, which showed dispersion with 0.5 wt% dispersant had the highest color strength. On the other hand, dispersion prepared with 0.75 wt% had the lowest color strength.

Difference between color strengths of dispersions with various dispersant concentrations can be explained by loss tangents at 10 Hz range of frequency sweep test.

Loss tangent of the reference sample prepared with 0.5 wt% dispersant was calculated as 0.63 and loss tangent of dispersant free dispersion was found 1.32. Dispersion containing 0.75 wt% dispersant had the highest loss tangent. Inverse relationship between loss tangent and color strength at 10 Hz was determined and is shown in Figure 6.5. Dispersions with highest loss tangent had the lowest color strength. Sedimentation was observed in dispersion with 0.25 wt% dispersant and color strength were not measured.

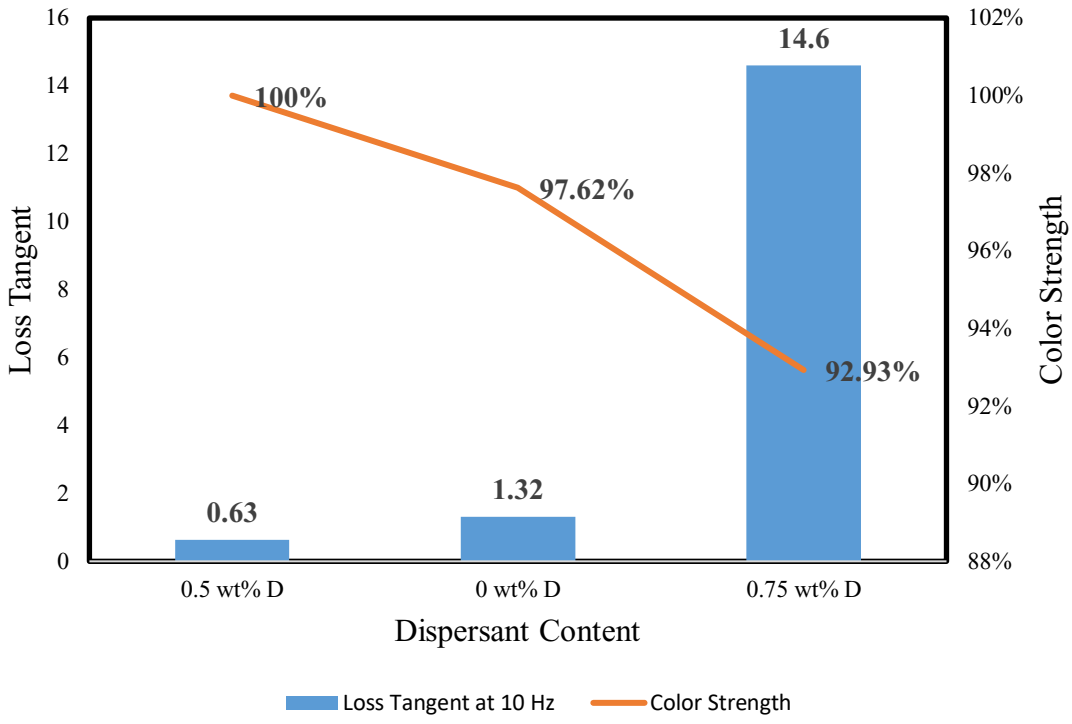

Figure 6.5. Dispersant Effect on Color Strength and Loss Tangent at 10 Hz

6.2. Pigment Content Effect on Rheological Properties of Carbon Black Dispersions

6.2.1.Pigment Content Effect on Viscosity

Effect of pigment content on steady shear rheology of dispersion containing carbon black was investigated and is shown in Figure 6.6. Viscosity was increased by

higher pigment content in the 0.01 s^{-1} to 100 s^{-1} range. Sample containing 30 wt% pigment had the highest shear thickening behavior at low shear rates. Dispersions containing 25 wt% and 27.5 wt% pigment also exhibited shear thickening behavior at low shear rates by orders of magnitude lower when compared to sample made with 30 wt% pigment content. After maximum viscosities, samples showed shear thinning behavior. Dispersions containing 30, 27.5 and 25 wt% pigment content had viscosities of 1.05, 0.61 and 0.37 Pa.s respectively at a shear rate of 100 s^{-1}. Maximum to minimum viscosity ratio was calculated as 11.78, 13.79 and 136.1 for dispersions prepared with 25, 27.5 and 30 wt% pigment contents respectively, and this indicates degree of shear thinning behavior was increased with pigment concentration. Dispersion prepared with 30 wt% pigment content had the highest degree of shear thinning behavior. This was related with higher particle interactions at low and moderate shear rates and breakdown of these interactions due to hydrodynamic forces at high shear rates.

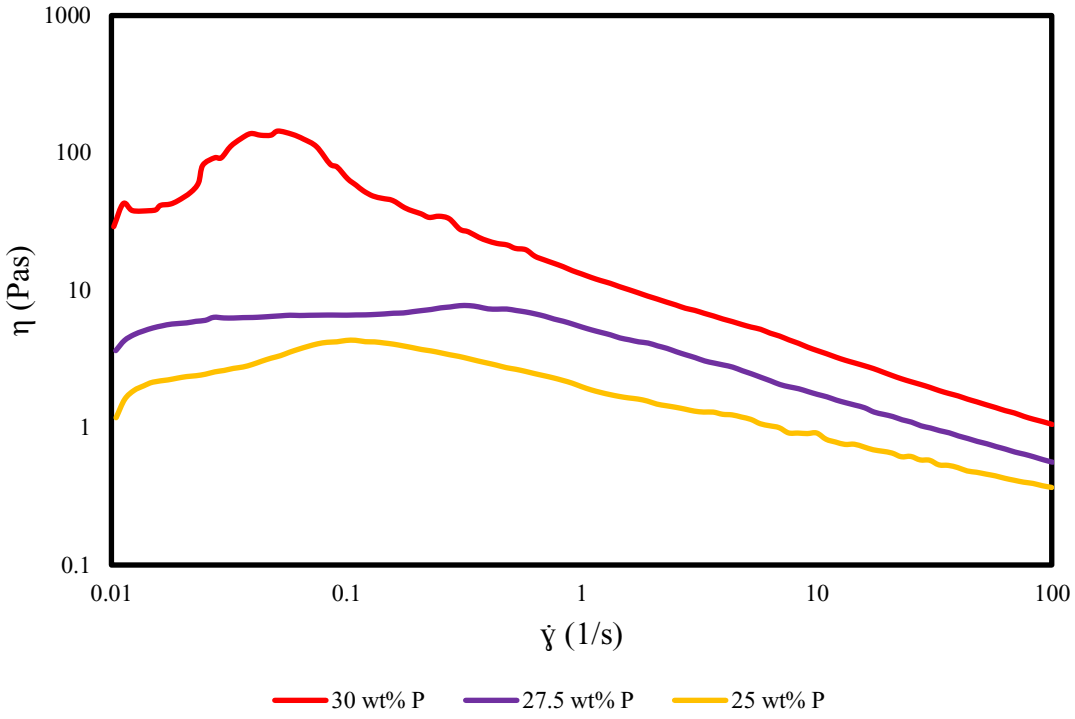

Figure 6.6. Pigment content effect on viscosity- shear rate graph of carbon black dispersions.

6.2.2. Pigment Content Effect on Dynamic Shear Rheology of Carbon Black Dispersions

Pigment content effect on dispersions was investigated by strain sweep test and can be seen in Figure 6.7. Increasing pigment content from 25 wt% to 30 wt% increased both G' and G'' which can be considered as an indication of improved particle interactions. G'' of dispersion containing 25 wt% pigment was higher than G'. At low strains, increase of pigment content to 27.5 wt% provided equality between G'' and G' at 0.2 strain which is called as cross-over point and larger strains than cross-over point provided higher G'' than G'. Dispersion prepared with 30 wt% pigment had higher G' than G'' until 0.27 strain while lowest pigment ratio containing sample never had G' dominant region. The rheological data indicated that higher solid contents resulted in greater cross-over points and shortened LVER of dispersions.

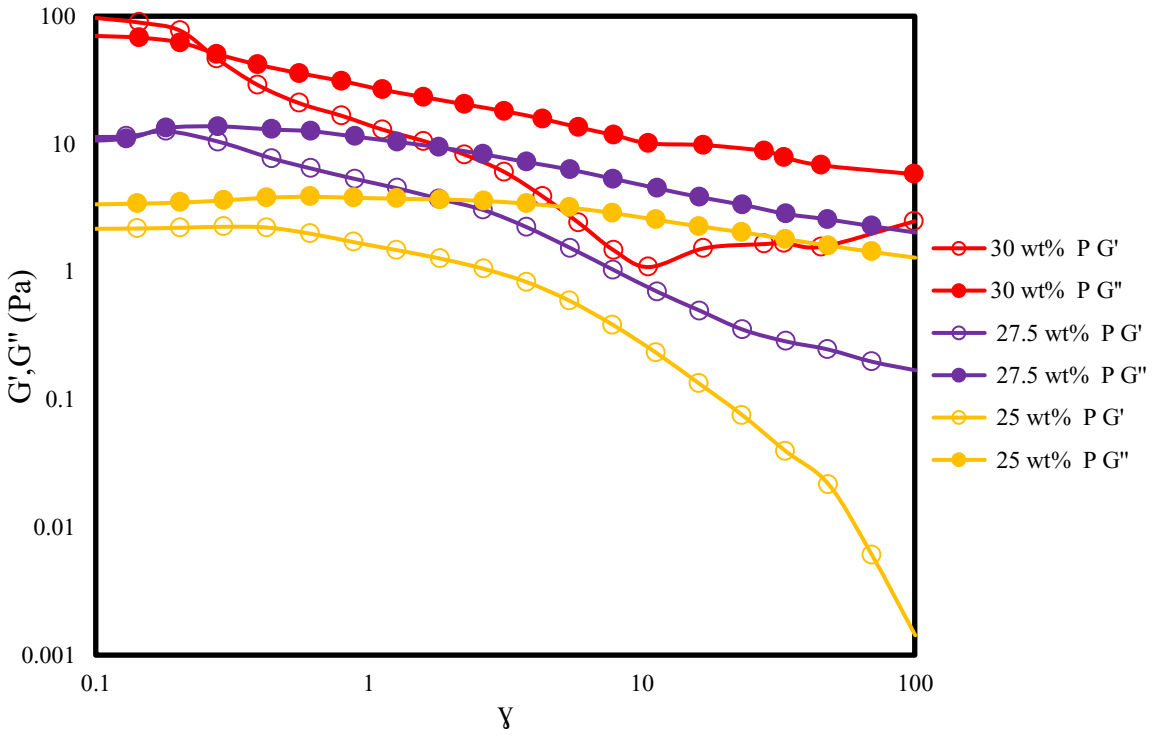

Figure 6.7. Pigment content effect on strain sweep graph of carbon black dispersion.

Frequency sweep measurements were performed with 0.2 strain. Frequency sweep tests of dispersions at 25 wt%, 27.5 wt% and 30 wt% pigment content are given in Figure 6.8. Both G' and G'' were frequency dependent and had descending behavior when frequency changed from 10 Hz to 0.1 Hz. G'' was higher than G' and was not dependent on solid content, and this showed more liquid-like behavior. At low frequencies that simulate long time range, 25 wt% pigment containing dispersion had the lowest G' value and indicating that sample had a weak network structure. Increasing pigment ratio resulted in higher G' and G''. There was only deviation of G' for 30 wt% and 27.5 wt% pigment containing samples and G' was seen as 6.54 and 12.37 Pa respectively at 0.1 Hz. This may be related to measurement error at low frequencies. At high (10 Hz) and medium (1 Hz) frequencies G' with 30 wt% pigment content was slightly higher.

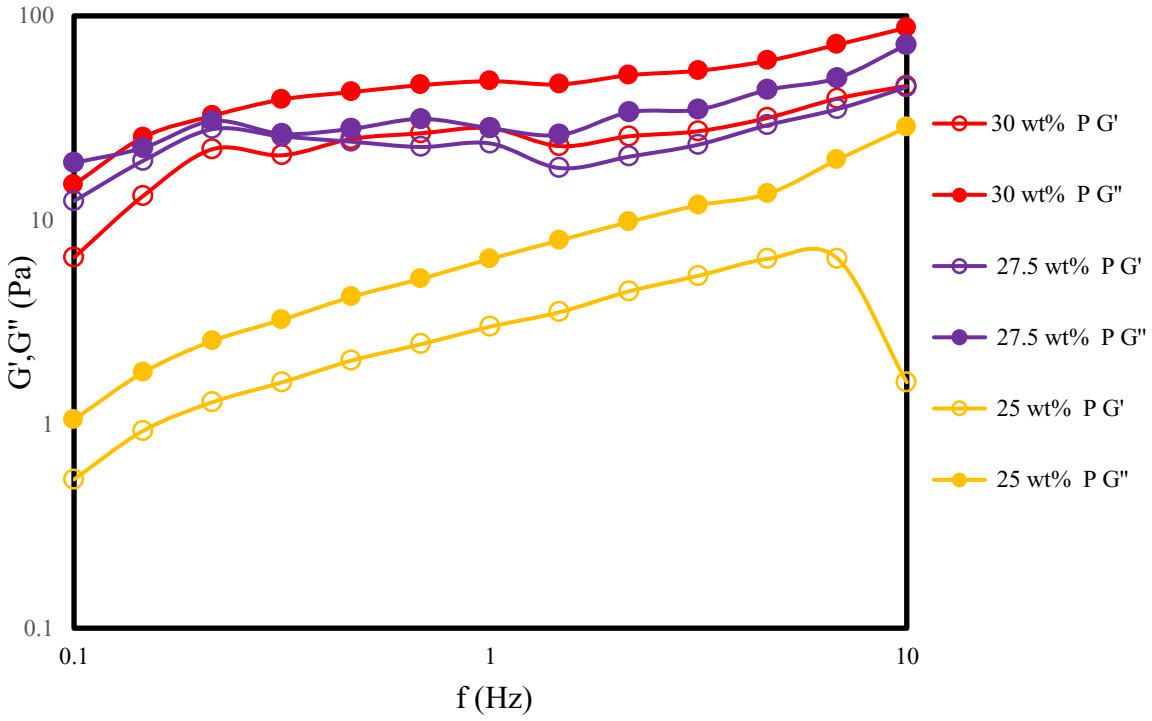

Figure 6.8. Pigment content effect on frequency sweep graph of carbon black dispersions.

6.2.3. Pigment Content Effect on Thixotropy

Pigment content effect on thixotropy was investigated and is shown in Figure 6.9. Thixotropic area of 25 wt%, 27.5 wt% and 30 wt% pigment containing dispersions were measured as 324, 544 and 1553 $Pa.s^{-1}$ respectively. There was a direct relationship between pigment content and thixotropic area. About a fivefold increase in thixotropic behavior was determined with 5 wt% increase of pigment content.

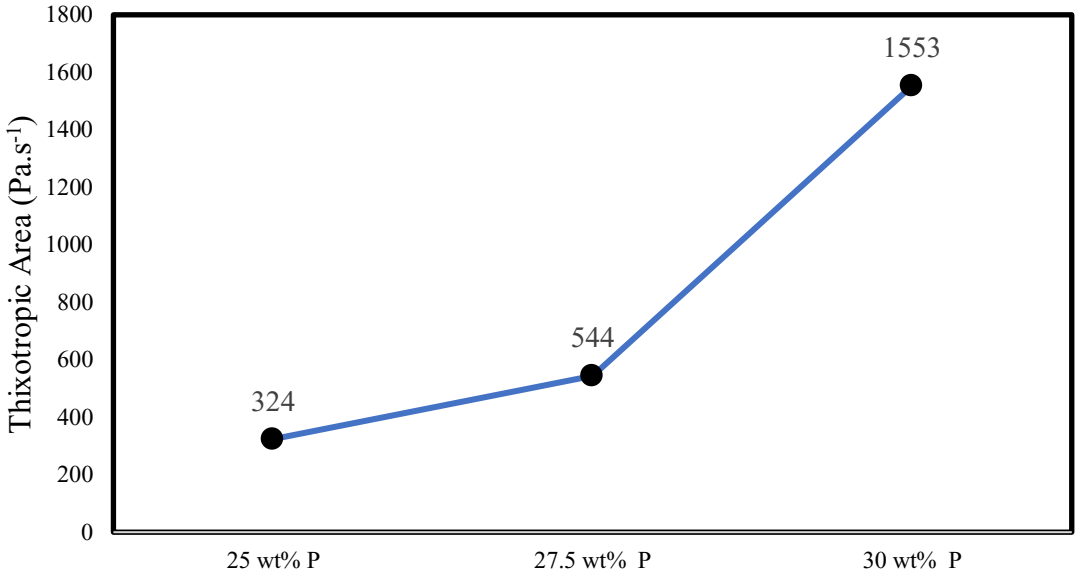

Figure 6.9. Hysteresis loop area (Thixotropy) comparison of dispersions prepared with 25 wt%, 27.5 wt%, 30 wt% pigment ratios.

6.2.4. Effect of Pigment Content Related Rheological Properties on Color Strength of Carbon Black Dispersions

Color strength measurements were done for samples prepared with 25, 27.5 and 30 wt% pigment containing samples and comparison with loss tangent at 10 Hz are shown in Figure 6.10. Ink containing 27.5 wt% pigment was selected as "reference sample". Color strength of inks with 27.5 wt% and 30 wt% pigment content was very close and higher than ink with 25 wt% pigment content. Difference between samples with 27.5 wt%

and 30 wt% pigment content was very low, and this was a surprise because expectation was to see higher color strength difference with 2.5 wt% pigment increase.

Maximum loss tangent at 10 Hz was observed at dispersion prepared with 25 wt% pigment content. On the other hand, loss tangent values at 10 Hz were recorded as 1.61 and 1.92 for dispersions with 27.5 wt% and 30 wt% pigment respectively. Color strength of dispersion with 27.5 wt% pigment content had lowest loss tangent and it was found weaker than 30 wt% pigment containing dispersion. This formed a contradiction with previous results and did not follow inverse relationship between color strength and loss tangent. Color strengths were very close to each other and difference between color strength values was only 0.68 %. Small differences disrupting the inverse relationship between color strength and loss tangent could be related with measurement error or evaporation of some solvent during rheology tests or color strength measurement.

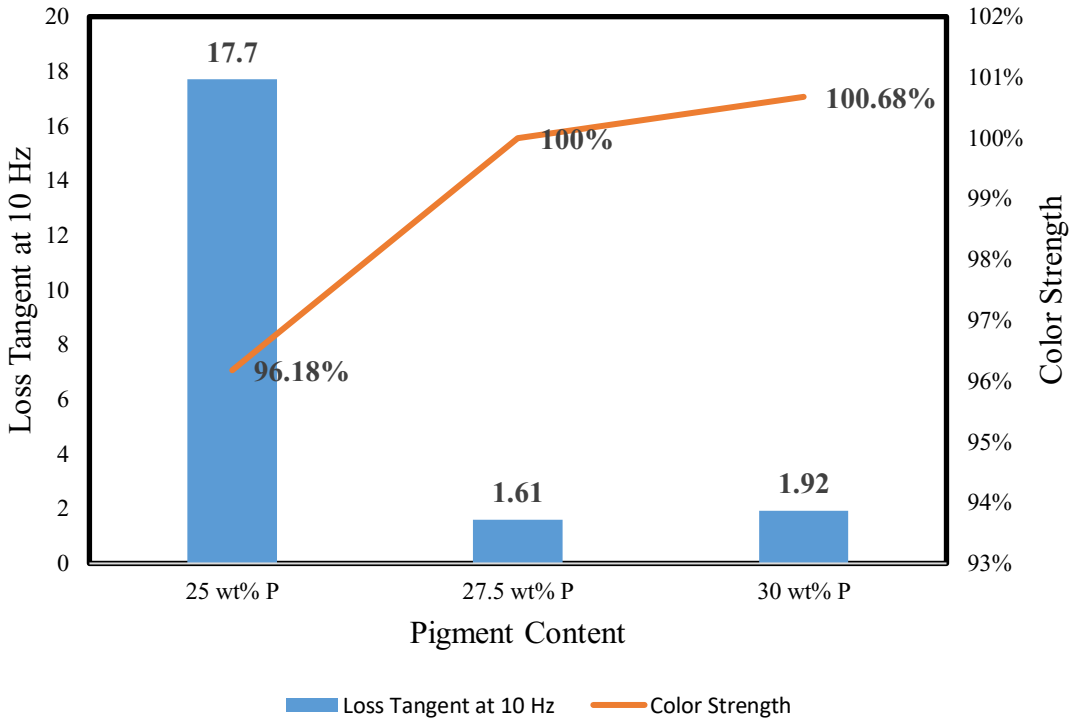

Figure 6.10. Pigment Content Effect on Color Strength and Loss Tangent at 10 Hz.

6.3. Varnish/Solvent Ratio Effect on Rheological Properties of Carbon Black Dispersions

6.3.1. Varnish/Solvent Ratio Effect on Viscosity

Effect of varnish/solvent ratio on the steady shear rheology of dispersions with 20 wt% pigment content was investigated and results are given in Figure 6.11. Ink prepared with highest V/S ratio of 2.2 had higher viscosity over entire range. Increase in varnish content led to the existence of excess non-adsorbed amount of polymer in continuous phase. Excess polymer contributed to the formation of a weak network structure between carbon black particles and increased the viscosities of the inks. All samples showed shear thinning behavior regardless of varnish to solvent ratio. The ratio of maximum to minimum viscosities at 0.01 s^{-1} and 100 s^{-1} was determined as 11.89, 5.99, 4.49, 4.49 for dispersions with V/S ratios of 1, 1.29, 1.67, 2.2 respectively.

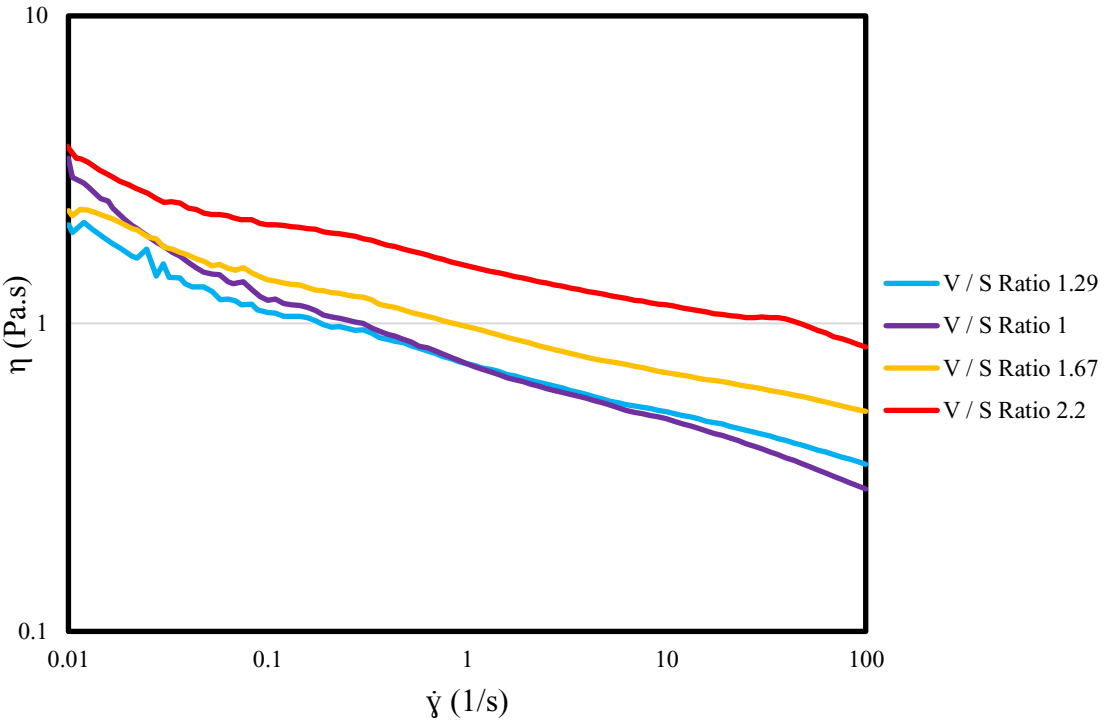

Figure 6.11. V/S ratio effect on viscosity- shear rate graph of carbon black dispersions

6.3.2. V/S Ratio Effect on Dynamic Shear Rheology of Carbon Black Dispersions

The strain sweep test was performed at a constant frequency of 1 Hz. Strain sweep test results of dispersions with different varnish to solvent ratios are shown in Figure 6.12. All samples had LVER, and microstructure remained constant until a critical strain value. Sample prepared with V/S ratio of 1 had the longest LVER that microstructure did not deform and G' was changed close to strain of 5. End of LVER was determined for dispersions prepared with 1.29, 1.67, 2.2 V/S ratios at 0.14, 0.63 and 0.2 ɣ respectively. Length of the LVER decreased as the weak network between the resin and the particles began to deform when V/S ratio was increased. LVER determined at 1.29 V/S was the only exception to this observation. G'' was dominant over G' for all samples.

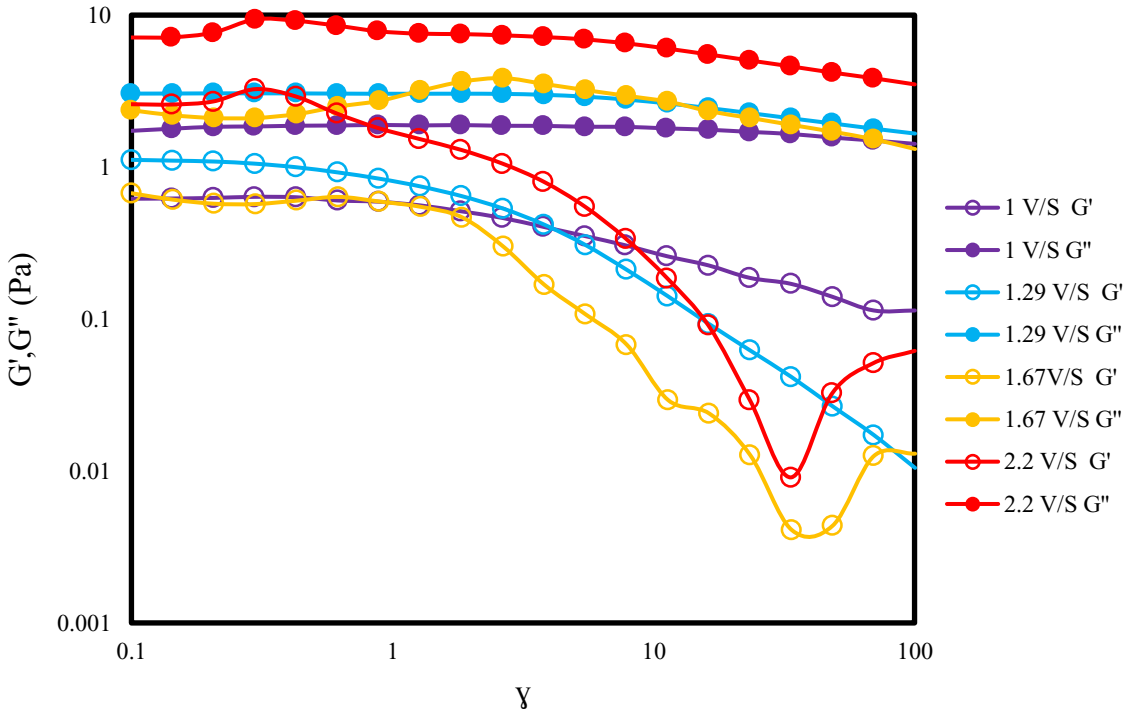

Figure 6.12. V/S ratio effect on strain sweep graph of carbon black dispersion

Frequency response is presented in Figure 6.13 with different V/S ratios at strain of 0.1. G'' was larger than G' for all dispersions, demonstrating dominant liquid like

behavior and all samples behaved frequency dependent. Increasing V/S ratio resulted in higher G' and G'' especially after V/S ratio of 1.29 at low frequencies. G' and G'' of inks with 1 and 1.29 V/S ratios had close values and loss tangents were similar. Loss tangent of dispersions with V/S ratio of 1, 1.29 and 1.67 was 3.17, 3.68 and 3.91 respectively at a relatively low 0.1 Hz frequency value. Dispersion with 2.2 V/S ratio had loss tangent value of 2.57 which was lower than other dispersions at low frequency. Loss tangent of dispersions was determined from highest to lowest for V/S ratios of 1.69, 2.2 ,1.29 and 1 with values as 6.32, 4.4, 2.36 and 1.08 respectively at 10 Hz.

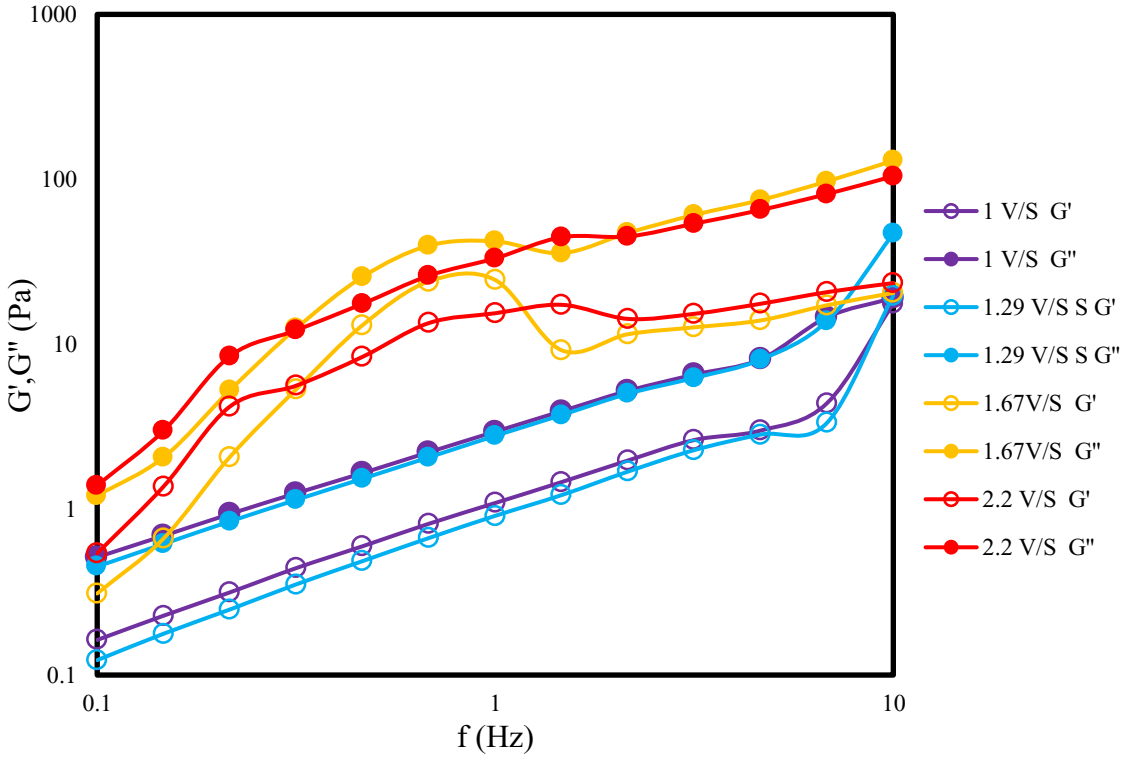

Figure 6.13. The frequency sweeps of dispersions prepared with 1, 1.29, 1.67 and 2.2 V/S ratios.

6.3.3. V/S Ratio Effect on Thixotropy

V/S ratio had an important effect on thixotropic behavior which is shown in Figure 6.14. At varnish solvent ratios of 1 and 1.29 thixotropic areas were very similar and were determined as 432 $Pa.s^{-1}$ and 431 $Pa.s^{-1}$ respectively. Increasing V/S ratio to 1.66 reduced thixotropic area to 343 $Pa.s^{-1}$. On the other hand, when the V / S ratio was 2.2, a significant

increase in thixotropy was observed and the highest thixotropic area was measured as 679 $Pa.s^{-1}$. Excess amount of varnish formed a weak network structure between particles, and this may be the reason for increased thixotropy due to changes in the stability of particles in varnish medium. Linear relationship between V/S ratio and thixotropic behavior wasn't determined and increase in V/S ratio above 1.29 resulted in thixotropy changes.

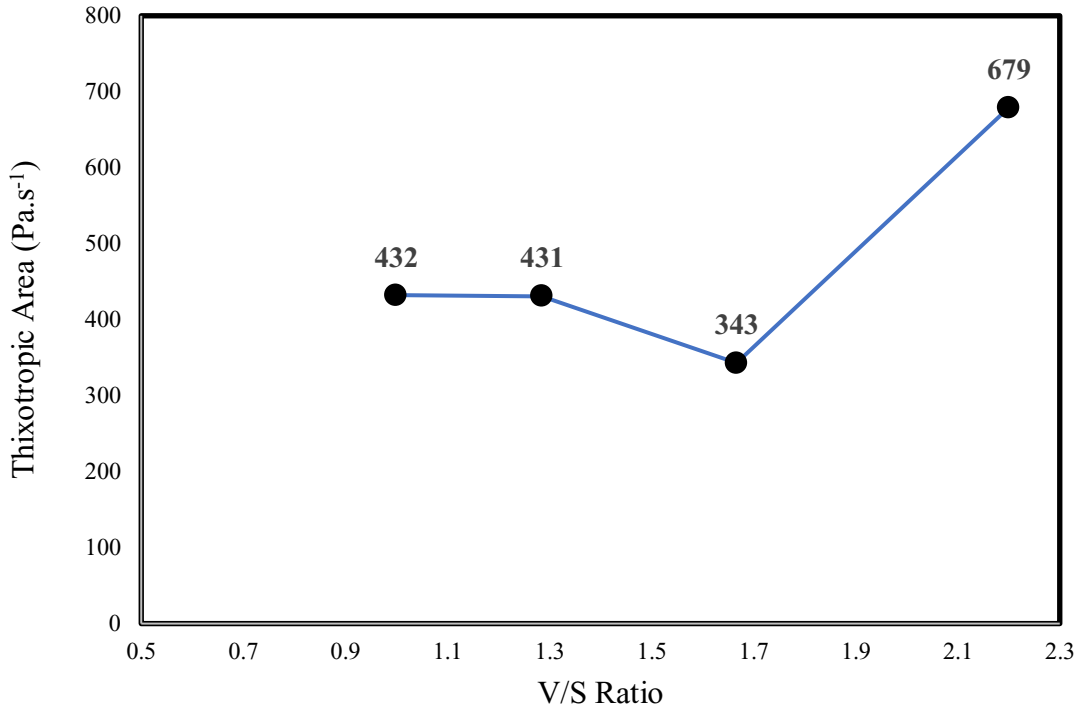

Figure 6.14. Hysteresis Loop Area (Thixotropy) of dispersions with V/S ratios of 1, 1.29, 1.67 and 2.2.

6.3.4. Effect of V/S Ratio on Rheological Property Related Color Strength of Carbon Black Dispersions

V/S ratio effect on color strength of printed inks and loss tangent at 10 Hz were analyzed and is shown in Figure 6.15. As reference sample dispersion prepared with V/S ratio of 1.67 was selected and color strength comparison was done according to that sample. According to Figure 6.12. dispersion having longest LVER with V/S ratio of 1 also had the highest color strength of 116.6 %. Color strength of other dispersions

prepared with V/S ratios of 1.29 and 2 was found as 107.22 % and 103.98 % respectively. This data showed that the increase in V/S ratio decreased the network strength of dispersions and color strength was reduced. Only exception was found at color strength of samples prepared with V/S ratio of 2.2, which had higher color strength than ink with V/S ratio of 1.67.

High frequency region especially close to 10 Hz reflects process conditions of printing. Loss tangents of dispersions with V/S ratios of 1, 1.29, 1.67 and 2.2 were measured 1.08, 2.36, 6.32 and 4.43 respectively. Dispersion prepared with 1.67 V/S had the highest loss tangent of 6.32 and color strength was weaker than other samples. Sample with V/S ratio of 1 that had the lowest loss tangent value was found stronger than other dispersions. V/S ratios above 1 resulted in weaker color strengths. Measurements have shown that color strength values were increased with decreasing loss tangent.

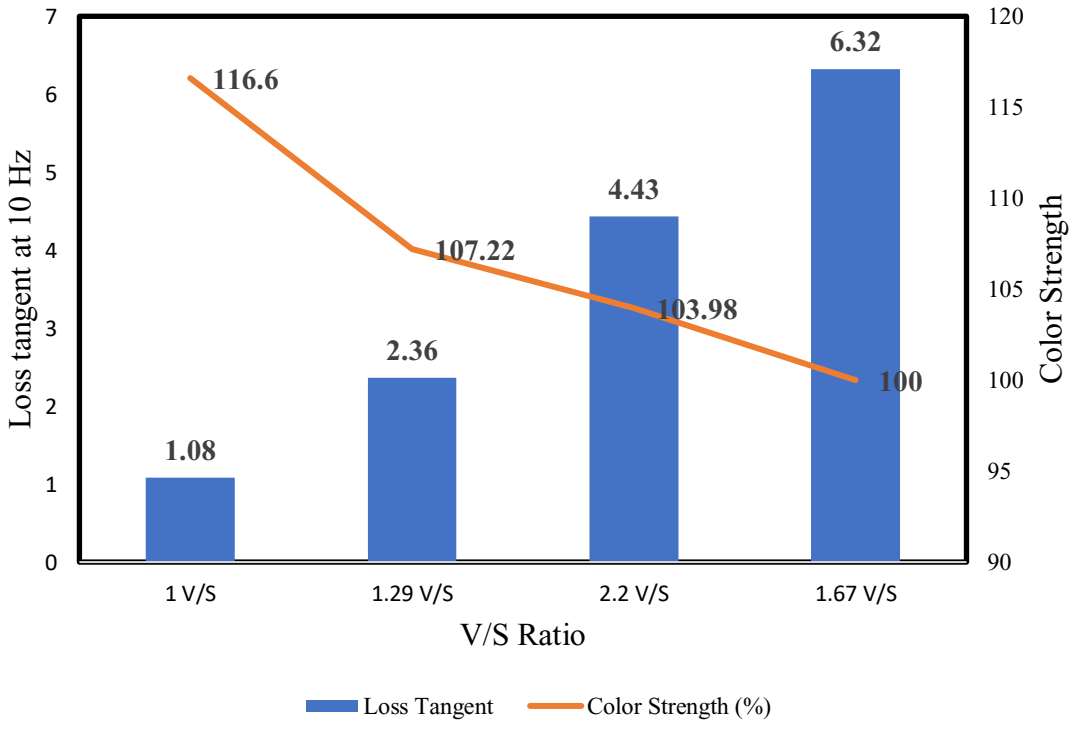

Figure 6.15. V/S Ratio Effect on Color Strength and Loss Tangent at 10 Hz.

6.4. Grinding Medium Effect on Rheological Properties of Carbon Black Dispersions

6.4.1. Particle Size Distribution of Dispersions Ground Different Mediums

Grinding with 0.5 mm and 0.8 mm yttrium stabilized beads was conducted and the particle size effect on rheological behaviors of carbon black dispersions with 20 wt% pigment content was investigated. Particle size distribution of samples ground with 0.5 mm and 0.8 mm is shown in Figure 6.16. As seen from the figure, dispersion ground with 0.5 mm beads had finer pigment particles compared to those ground with 0.8 mm beads. The high intensity peaks in the distributions were reduced from 0.8 μm to 0.1 μm with the decrease in grinding medium size from 0.8 mm to 0.5 mm. The biggest particles present in the samples (D_X 100) were 5.17 μm and 35.1 μm for 0.5 mm and 0.8 mm ball media ground samples respectively. This result showed decrease of largest pigment particles with grinding lower sized medium. Average volumetric particle sizes for dispersions ground with 0.5 mm and 0.8 mm beads were measured as 0.244 μm and 0.890 μm respectively. Span width of dispersions ground with 0.5 mm and 0.8 mm beads were 2.94 and 2.55 respectively.

Dispersions ground with 1.3 mm glass beads had coarser particle size distribution than inks ground with 0.5 mm and 0.8 mm beads. Highest peak was observed close to 1 μm for dispersions ground with 1.3 mm beads and small peak was observed close to 0.1 μm. Volume density of highest peak was also larger than peaks of dispersions ground with 0.5 and 0.8 mm beads. Increasing grinding medium size resulted in coarser particle distributions for dispersions and highest peaks were passed to smaller sizes.

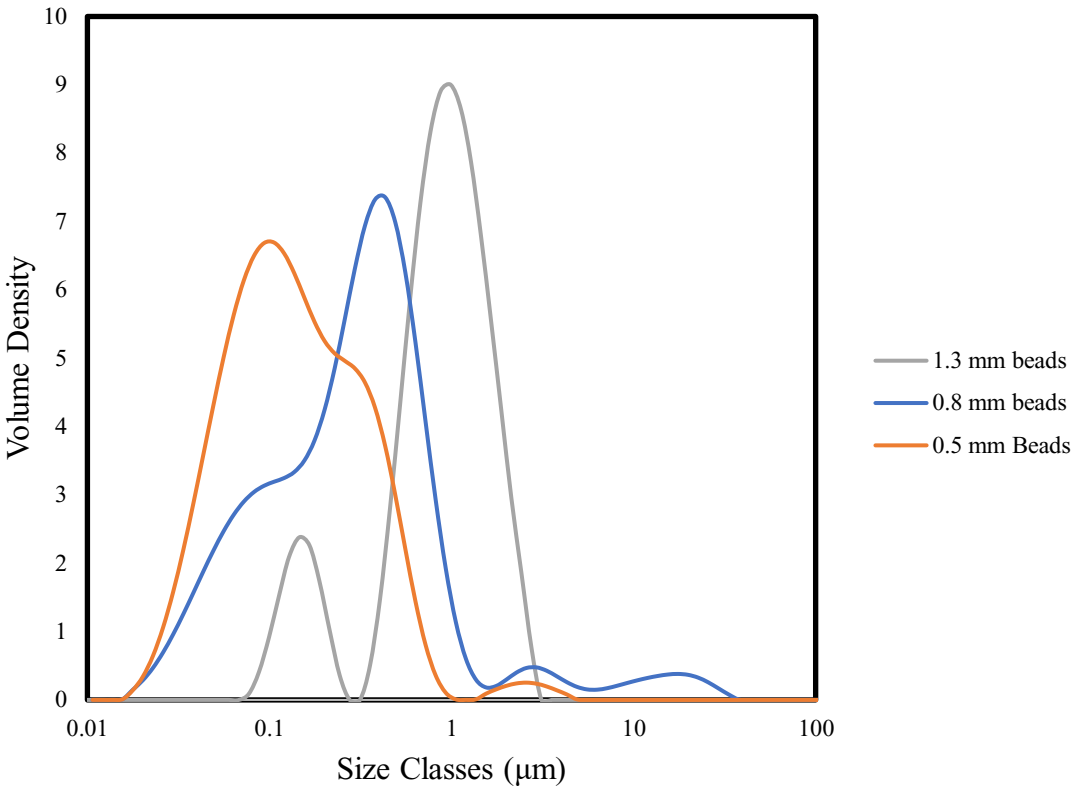

Figure 6.16. Particle size distribution of dispersions ground with 0.8 mm and 0.5 mm beads

6.4.2. Grinding Medium Effect on Viscosity

Effect of grinding medium and particle size distribution on the viscosity of carbon black dispersions was investigated and is shown in Figure 6.17. Two different sizes of yttrium stabilized zirconia beads of 0.5 mm and 0.8 mm sizes were used as grinding medium. There was no viscosity difference between dispersions ground with 0.8 mm and 0.5 mm beads at 0.01 s^{-1}. Dispersion ground with 0.8 mm beads had shear thickening behavior until 0.1 s^{-1} and after that value, shear thinning behavior started while dispersion ground with 0.5 mm beads had shear thinning behavior over the entire range. Dispersion with finer size distribution which was ground with 0.5 mm had lower viscosities over the entire shear rate range. Viscosity difference between 0.5 mm and 0.8 mm ground samples could be explained by particle sizes and packing behavior. Presence of higher amounts of finer particles provided shear thinning behavior for 0.5 mm ground sample. This result

could be related with filling of the pores between larger particles with smaller particles and decrease in interaction between larger particles during flow.

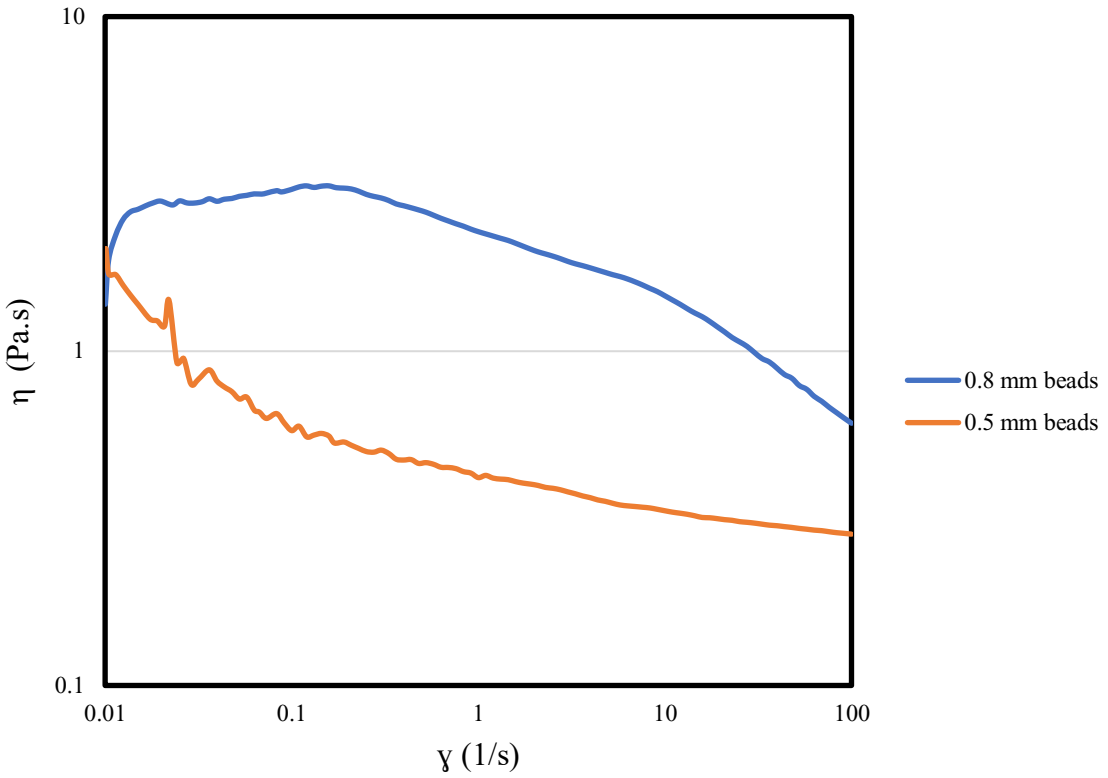

Figure 6.17. Viscosity- shear rate graph of dispersion ground with 0.8 mm and 0.5 mm beads

6.4.3. Griding Medium Effect on Dynamic Shear Rheology

Grinding medium bead size and dispersion particle size effect on dynamic rheological properties are shown in Figure 6.18. Regardless of the grinding medium, G" in both samples was dominant over G'. Dispersion ground with 0.5 mm beads with finer size distribution had lower G'' and G' than dispersion ground with 0.8 mm that had coarser size distribution. This behavior can be related with the fitting of small particles between larger particles hence reducing particle interactions. In terms of both dispersion's LVER, important difference was not observed.

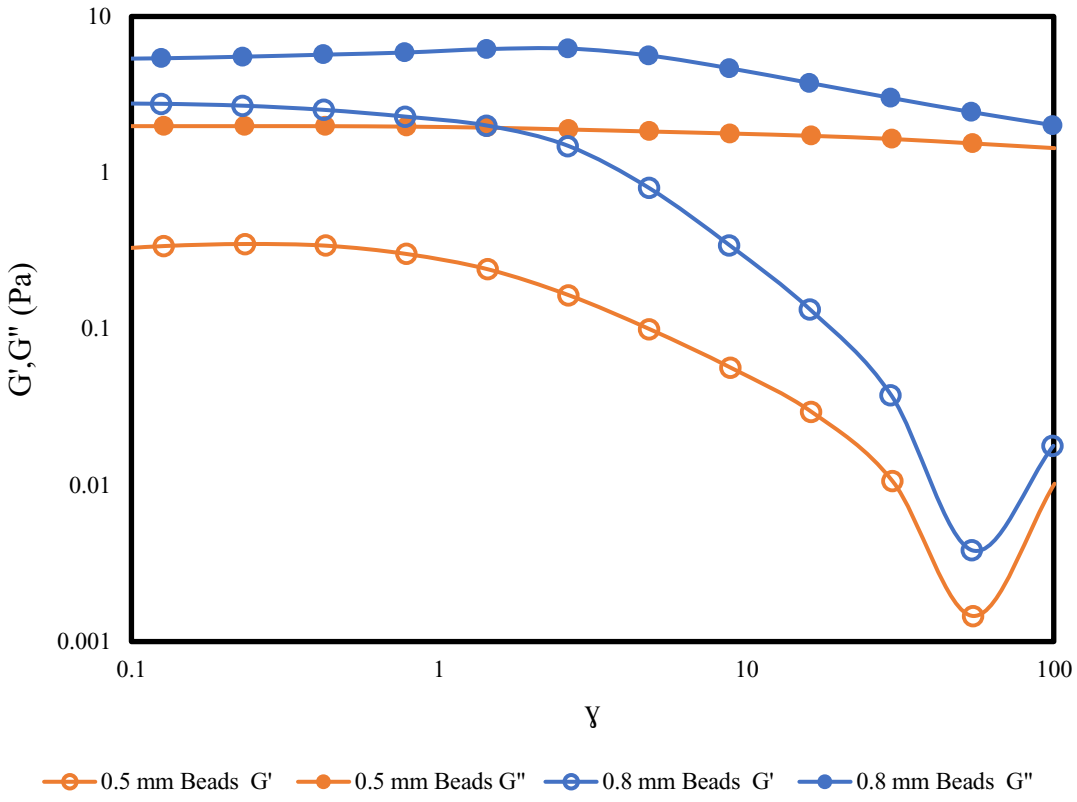

Figure 6.18. Strain sweep graph of dispersions ground with 0.8 mm and 0.5 mm beads

Frequency sweep curves of inks ground with 0.5 mm and 0.8 mm is shown in Figure 6.19. At low frequencies below 1 Hz, G' of samples ground with 0.8 mm were higher than G'' and cross-over was observed close to 1 Hz. Beyond that point G'' became dominant over G'. Grinding with finer beads resulted in lower G' and G'' all over the range. In frequency range, both G' and G'' decreased with decreasing frequency. G' and G'' of dispersion ground with bigger sized beads decreased about 40 times, while grinding with small sized beads had a reduction ratio of 300 times. At 0.1 Hz and 10 Hz, dispersion ground with 0.8 mm beads had loss tangent close to 1 while dispersion ground with 0.5 mm beads had higher values.

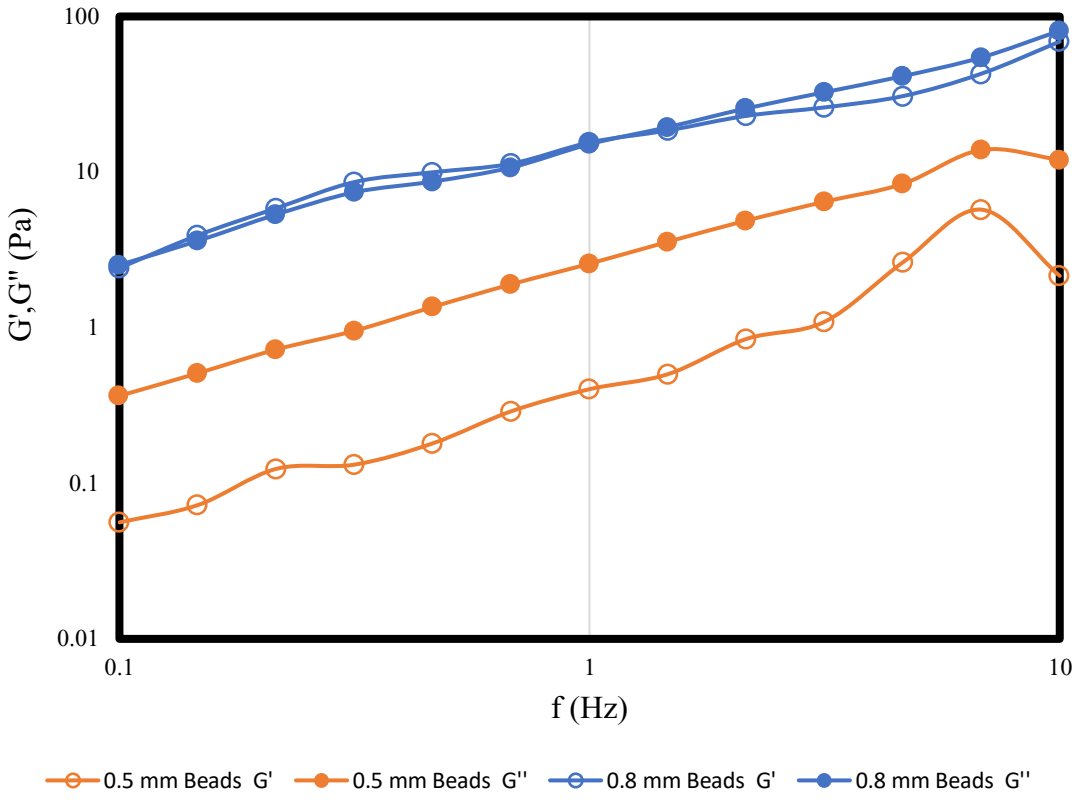

Figure 6.19. Frequency sweep graph of dispersions ground with 0.5 mm and 0.8 mm beads

6.4.4. Grinding Medium Effect on Thixotropy

Thixotropic behavior of dispersions ground with 0.5 mm and 0.8 mm beads is given in Figure 6.20. Dispersion ground with 0.5 mm beads had 213 $Pa.s^{-1}$ while dispersion ground with 0.8 mm beads had 1041 $Pa.s^{-1}$. This showed that the dispersion with coarser particle size distribution had about 5 times higher thixotropy than dispersion with smaller particle size distribution. Structure of dispersion with larger particle size distribution recovered in longer time than dispersion with smaller particle size distribution.

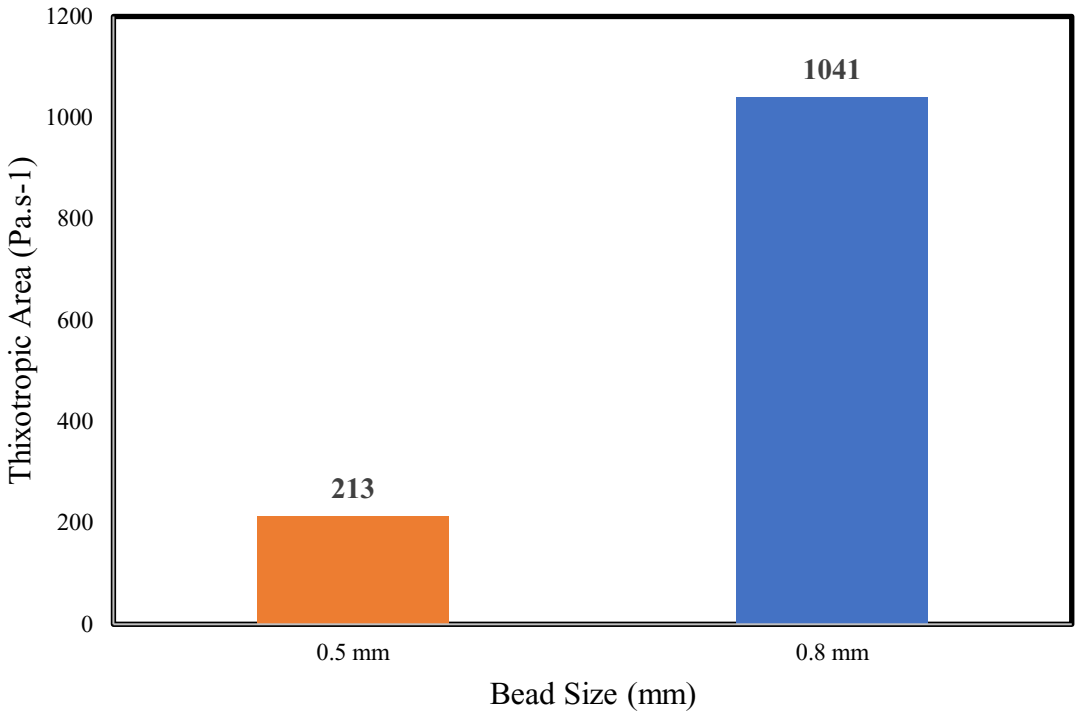

Figure 6.20. Hysteresis Loop Area (Thixotropy) comparison of dispersions ground with 0.5 mm and 0.8 mm beads.

6.4.5. Grinding Medium Effect on Rheological Property Related Color Strength of Carbon Black Dispersions

Grinding medium bead size has an important effect on particle size reduction and distribution. Figure 6.16 shows grinding with smaller bead size had more efficient particle size reduction. Grinding medium, loss tangent and color strength relationship is shown in Figure 6.21. Dispersion ground with 0.8 mm beads was selected as reference sample and color strength was assumed as 100 %. Dispersion ground with 0.5 mm beads had about 7 % weaker color strength compared to 0.8 mm ground dispersion.

Dispersion ground with 0.8 mm had loss tangent of 1.17 while 0.5 mm ground had 5.5 loss tangent at frequency of 10 Hz. Color strength of 0.5 mm ground dispersion with higher loss tangent was found % 7 weaker. This result indicated a similar behavior with previous findings and dispersions with lowest loss tangent had the highest color strength.

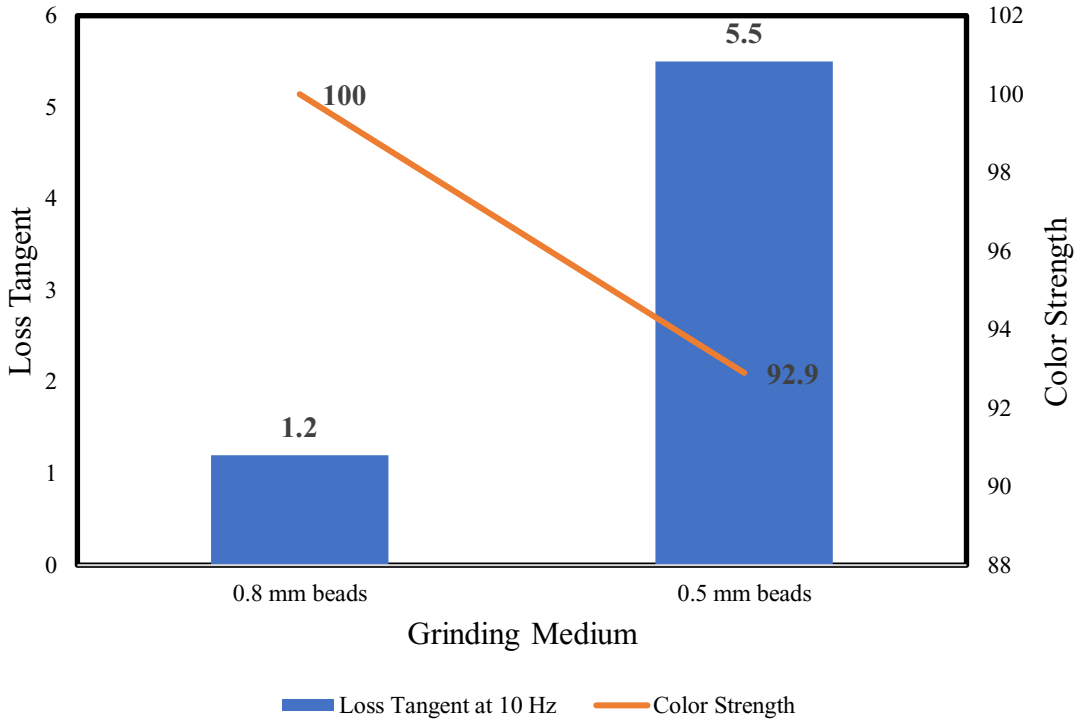

Figure 6.21. Grinding Medium Effect on Color Strength and Loss Tangent at 10 Hz.

6.5. Grinding Time Effect on Rheological Properties of Carbon Black Dispersions

6.5.1. Grinding Time Effect on Viscosity

Distribution of pigment particles in dispersion uniformly can be achieved by grinding. In addition to grinding medium, grinding time is also an important parameter that affects the dispersion state. Viscosity of dispersions ground for 30 and 60 minutes with pigment contents of 20 wt% and 25 wt% were examined and are given in Figure 6.22. Samples containing 20 wt% pigment showed shear thinning behavior and no variation was observed with increasing grinding time. Dispersions containing 25 wt% pigment contents had higher viscosity over the shear rate range and behaved shear thickening until 0.2 s^{-1}. Beyond that point they also exhibited shear thinning behavior. When inks prepared with 25 wt% pigment contents were compared, viscosity of 60

minutes ground ink was higher than 30 minutes ground ink. Ratio of maximum viscosity to minimum viscosity was calculated as 11.7 and 18.4 for 30 minutes and 60 minutes ground samples at 25 wt% pigment content. This showed that an increase in grinding time increased the degree of shear thinning behavior. When milling time was increased to 60 minutes, remaining aggregated carbon black particles were better dispersed. This formed more contact points between particles and increased viscosity.

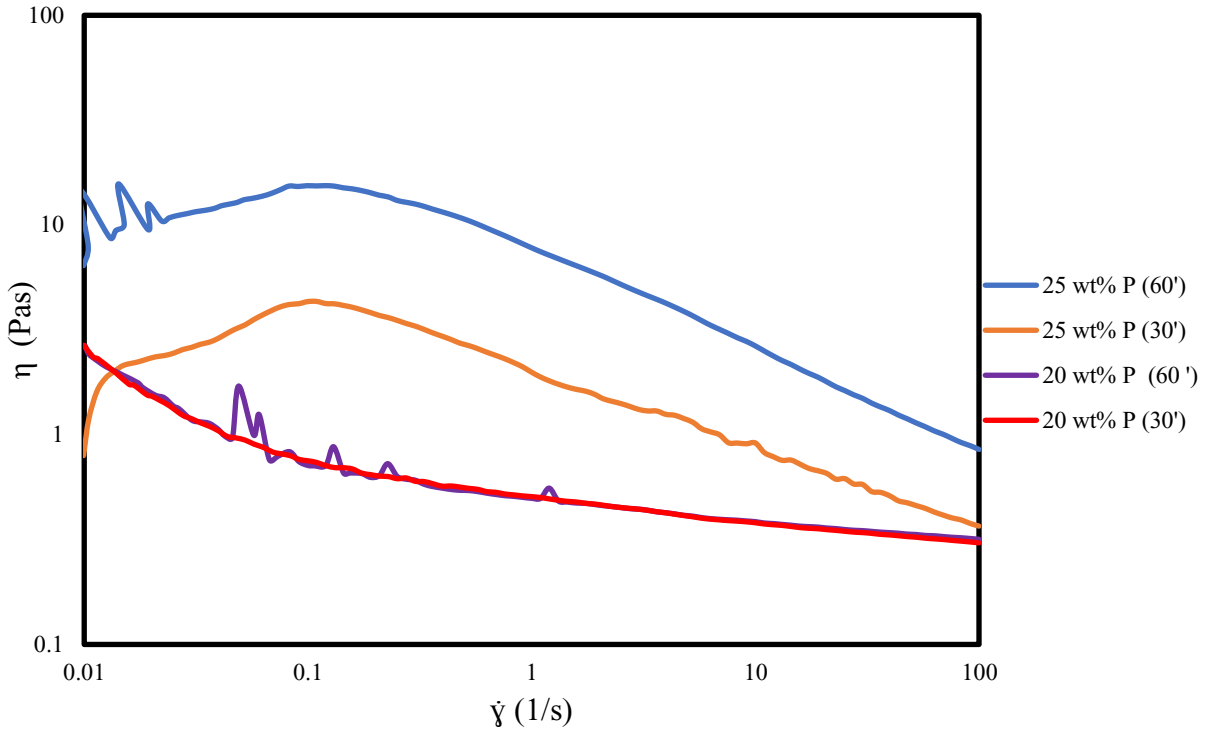

Figure 6.22. Viscosity shear rate graph of grinding time effect on dispersions containing 20 wt% and 25 wt% pigment contents.

6.5.2. Grinding Time Effect on Dynamic Shear Rheology

Viscoelastic responses of dispersions at different grinding times were investigated and are shown in Figure 6.23. G'' was found higher than G' for all samples over entire range. Grinding time increase from 30 to 60 minutes resulted in greater G' and G'' at higher pigment content. G' of 25 wt% pigment containing sample with 60 minutes grinding was about 4 times higher than 30 minutes ground sample at low strains. Samples

with low pigment ratios had the same G' and G" in whole range, regardless of grinding time. LVER increased with grinding time for samples with 25 wt% pigment, while low pigment containing samples had close LVER at different grinding times.

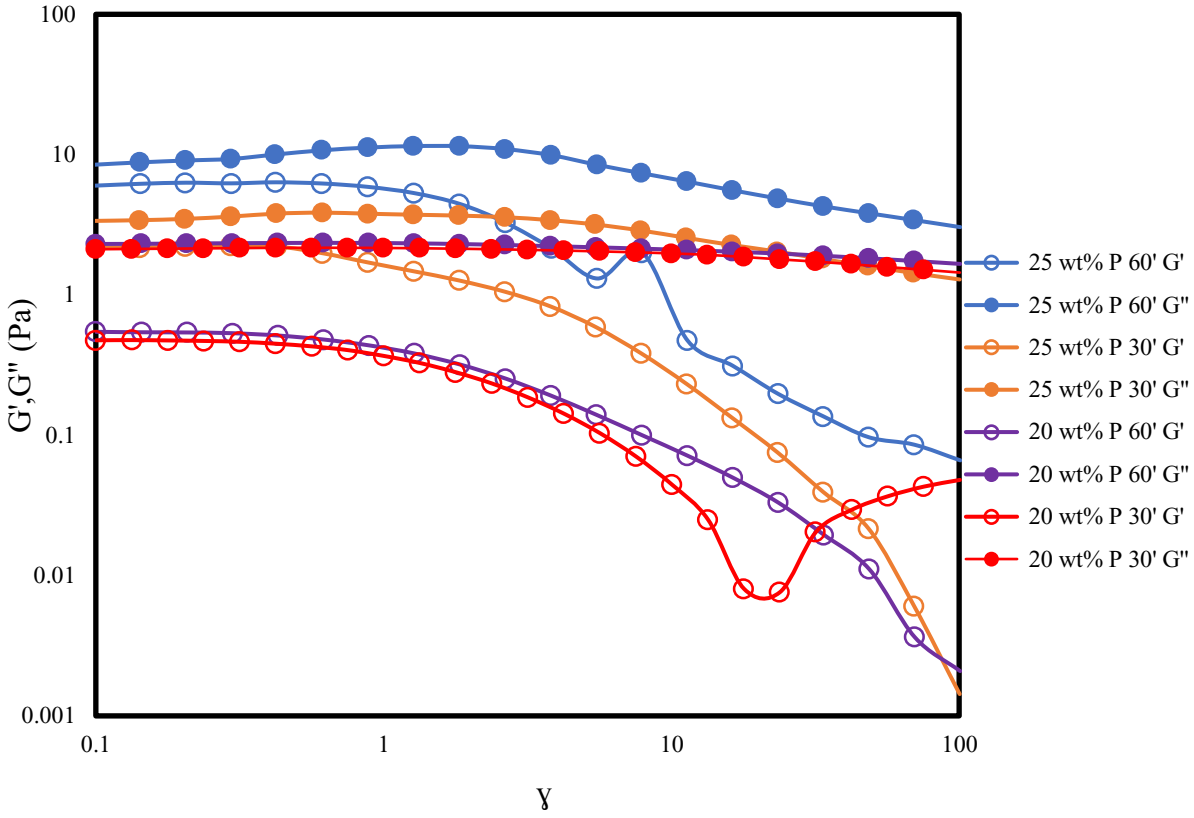

Figure 6.23. Strain sweep graph of grinding time effect at 20 wt% and 25 wt% pigment contents.

Frequency sweep tests were performed for viscoelastic behavior of dispersions prepared at 20 and 25 wt% pigment contents with 30/60 minutes grinding. G’ and G’’ variation with frequency is shown in Figure 6.24. In the investigated range, G’’ was higher than G’ and this was an indication of liquid-like behavior. Ink ground 60 minutes with 25 wt% had the highest G’ and G’’ which was consistent with previous results due to the network structure. Dispersions containing 20 wt% pigment content had lower values of both G’ and G’’ than dispersion with 25 wt% pigment content. Grinding effect on G’ and G’’ of lower pigmented dispersions was negligible and their plots overlapped.

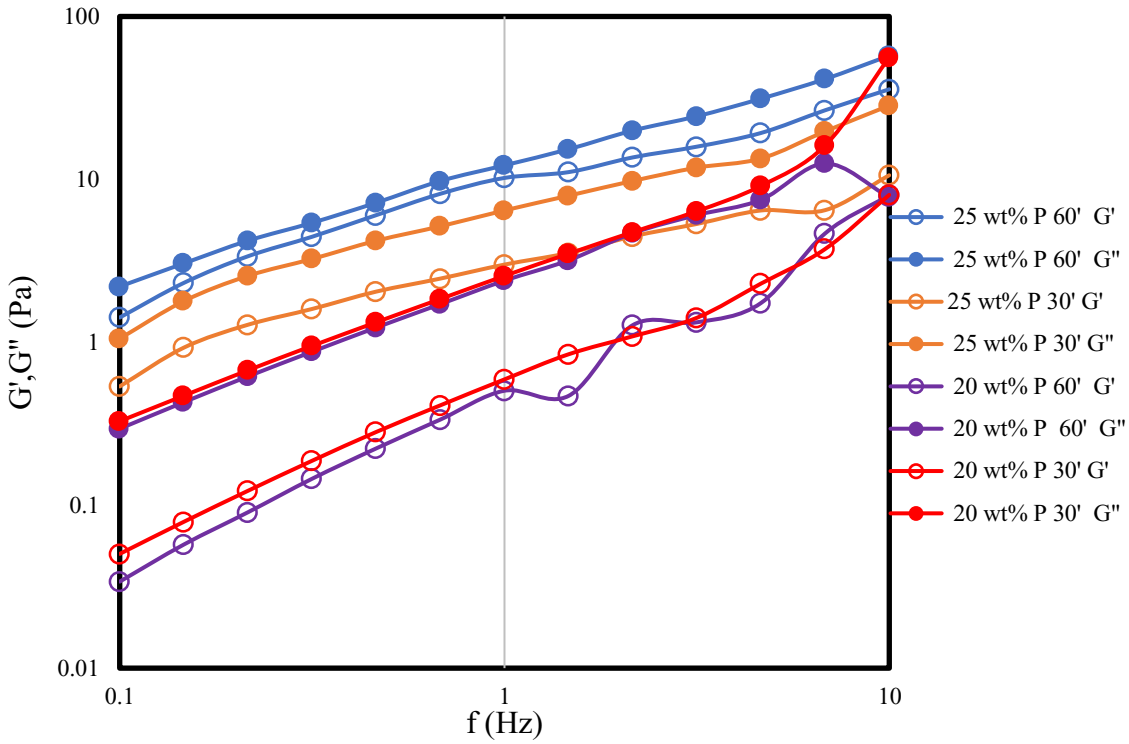

Figure 6.24. Frequency sweep graph of grinding time effect at 20 wt% and 25 wt% pigment content.

6.5.3. Grinding Time Effect on Thixotropy

Figure 6.25 shows grinding time effect on thixotropy at pigment ratios of 20 wt% and 25 wt%. After 30 and 60 minutes of grinding, thixotropy of inks made with pigment content of 20 wt% were close to each other and were measured as 268 $Pa \cdot s^{-1}$ and 184 $Pa \cdot s^{-1}$ respectively. Difference between them was not so high and this result showed that grinding more than 30 minutes did not change the dispersion state drastically at low pigment content.

Samples prepared with 25 wt% pigment content had higher thixotropy compared to lower pigment containing samples. One of the reasons behind that result was related to network structure formation. Due to the presence of a larger number of particles/close contacts between particles with higher pigment content the structure recovers in a longer time. Ink sample ground 60 minutes with 25 wt% pigment content had almost 4 times higher thixotropy than 30 minutes ground sample.

.

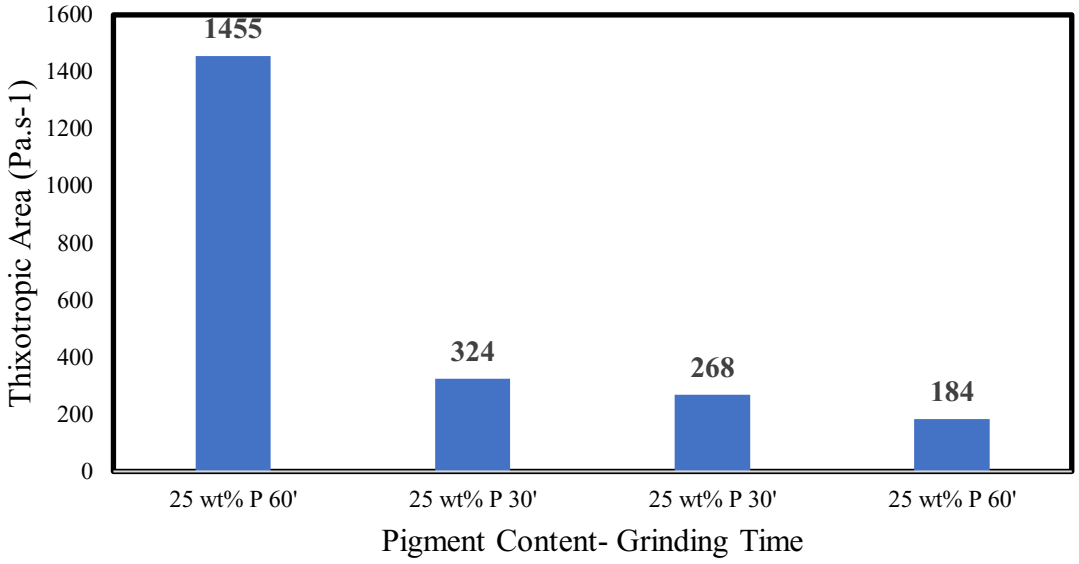

Figure 6.25. Hysteresis Loop (Thixotropy) of dispersion at 20 wt% and 25 wt% pigment content with 30 minutes and 60 minutes grinding.

6.5.4. Effect of Grinding Time on Rheological Property Related Color Strength of Carbon Black Dispersions

Grinding time effect on color strength and 10 Hz loss tangent of dispersions at 20 wt% and 25 wt% pigment content was investigated and is shown in Figure 6.26. Dispersion prepared with 20 wt% pigment, 60 minutes grinding was selected as reference. As seen from figure, independent of the grinding time samples prepared with higher pigment content had stronger color strength. Grinding time increase from 30 to 60 minutes enhanced color strength 15 % at 25 wt% pigment containing dispersions. Grinding time effect became more dominant over color strength at higher pigment contents due to higher amounts of collisions between particles and beads. Grinding time increase effect was found minimum at 20 wt% pigment containing samples and color strength of those two inks were similar and close to 100 %.

Relationship between the loss tangent and the color strength was investigated and is shown in Figure 6.26. Dispersion with 20 wt% pigment content and 30 minutes

grinding had highest loss tangent of 6.9 at 10 Hz and color strength of that ink was weaker than other dispersions. 20 wt% pigmented and 60 minutes ground dispersion had the lowest loss tangent value of 0.97 and was weaker than dispersion containing 20 wt% pigment with 30 minutes grinding. This was incompatible with previous color strength and loss tangent results. This result can be explained by some measurement errors at high frequencies for that sample. 25 wt% pigment containing dispersions ground for 30 and 60 minutes had loss tangent values of 2.7 and 1.6, respectively. Increase of grinding time resulted in lower loss tangent and higher color strength for 25 wt% pigment containing dispersions.

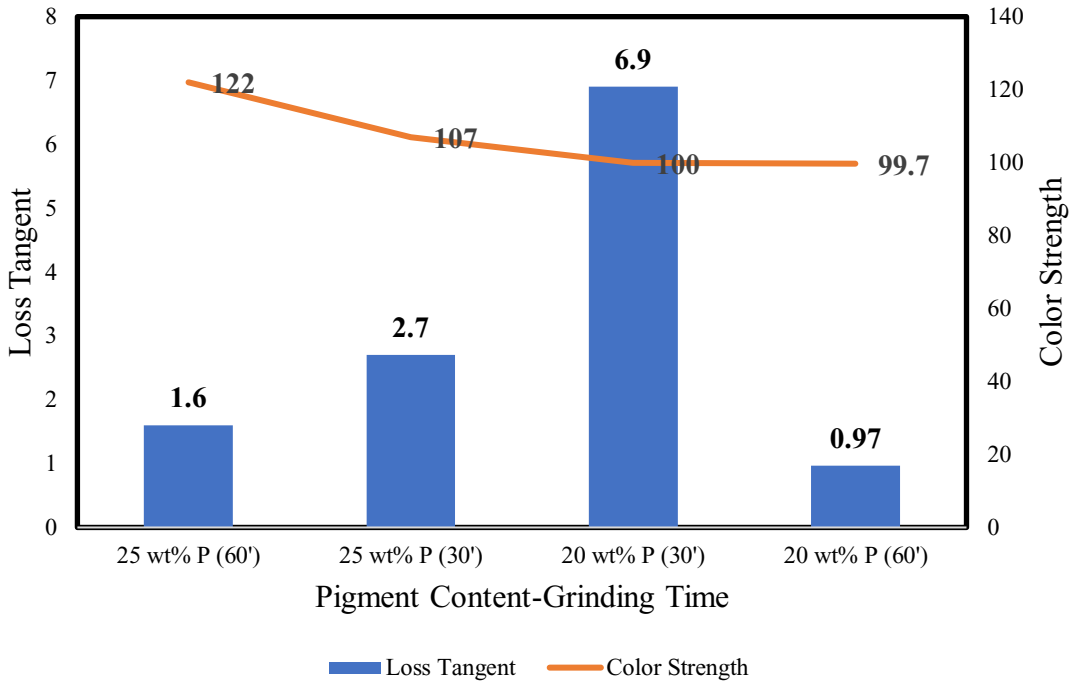

Figure 6.26. Grinding Time Effect on Color Strength and Loss Tangent at 10 Hz.

6.6. Storage Period Effect on Rheological Properties of Carbon Black Dispersions

6.6.1. Storage Period Effect on Viscosity

Dispersion with and without dispersant were prepared and their viscosities were measured freshly and after three months storage period for the determination of the

influence of dispersant on stability/shelf life for three months. Figure 6.27 shows that all dispersions had shear thinning behavior independent of storage time and dispersant ratio. Sedimentation wasn't determined in all the samples. Viscosity measurements conducted on inks after three months storage period resulted in similar with the freshly prepared ink viscosity by using dispersant. This may be directly related to the adsorption of the dispersant, formation of network structure and stability. Significant storage period effect on viscosity was observed for samples prepared without dispersant. Viscosities of dispersant free inks were found 0.3 Pa.s and 0.46 Pa.s for measurements completed freshly and after three months storage period at 100 s^{-1}. This was an indication of agglomeration of particles due to lack of stability and viscosity increased with the formation agglomerates in inks during storage.

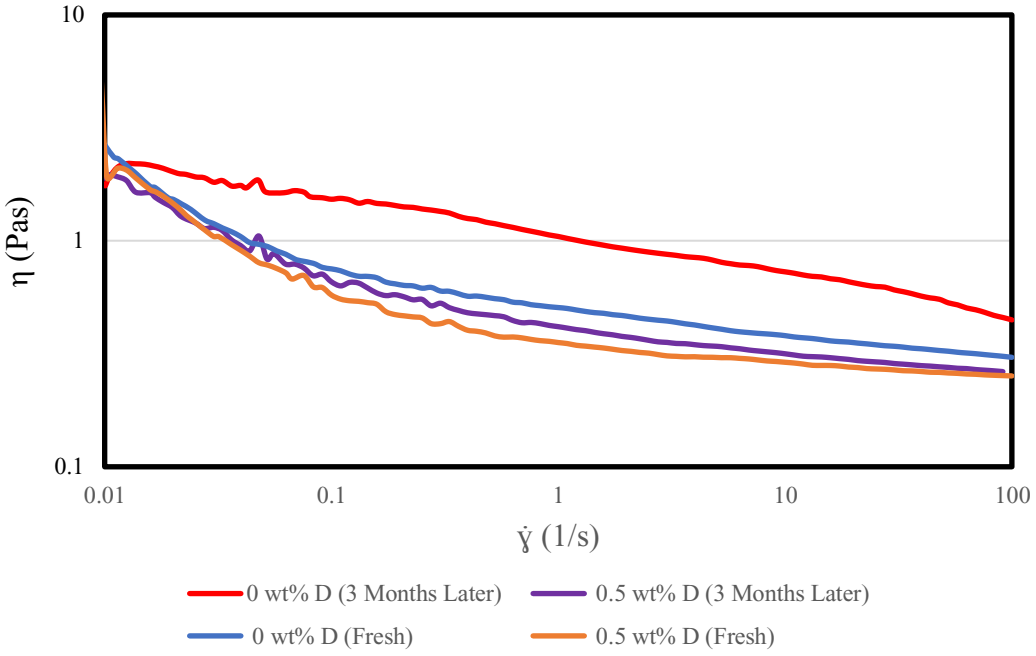

Figure 6.27. Storage period effect on viscosity shear rate measurements of dispersions with 0 wt% D and 0.5 wt% D during 3 months.

6.6.2. Storage Period Effect on Dynamic Shear Rheology

Strain sweep test was performed to extract information regarding storage period effect on viscoelastic properties of dispersions with and without dispersant and is shown in Figure 6.28. G'' was dominant over G' for all samples. Sample prepared without

dispersant and measured after three months storage period had the lowest LVER, but no significant difference was observed between LVERs of other samples. Having small LVER could be related with broken flocculates with higher strains. G' of dispersant containing inks changed from 0.23 Pa to 0.42 Pa at strain of 0.1 during storage period. G' was deviated from 0.47 to 1.5 at 0.1 ɣ. G' of the dispersant free dispersion increased at a higher rate than the dispersant containing ink during storage period.

According to frequency sweep tests, G'' was dominant over G' all over the frequencies which showed liquid like behavior. Figure 6.29 shows variations of G' and G'' with storage period and dispersant content.

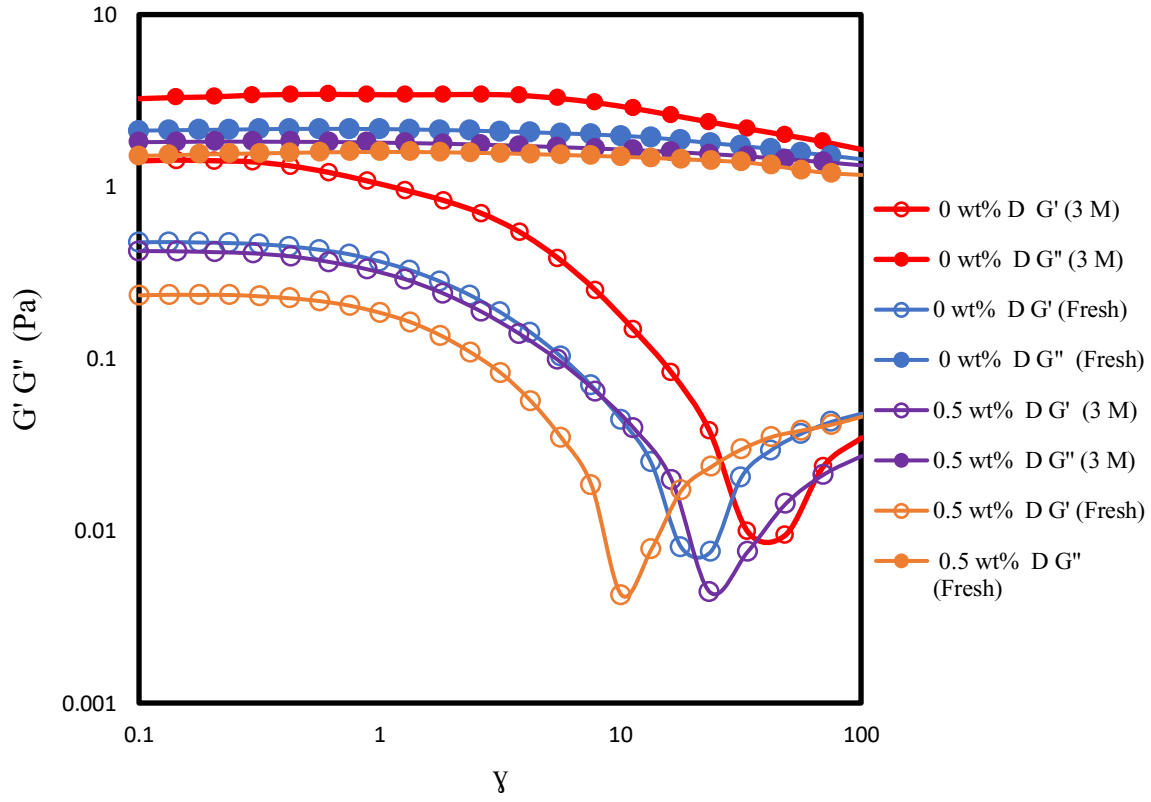

Figure 6.28. Strain sweep graph of storage period effect on dispersions with 0 wt% D and 0.5 wt% D.

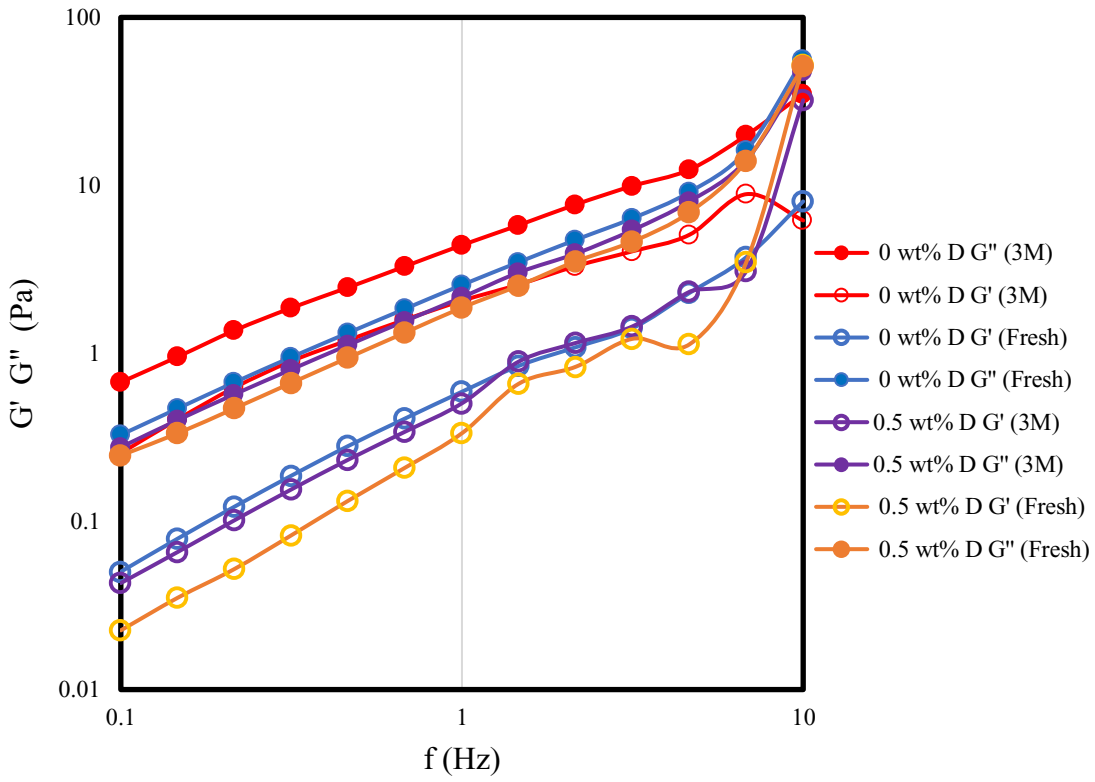

Figure 6.29. Frequency sweep graph of storage period effect on dispersions with 0 wt% D and 0.5 wt% D.

Loss tangent of the dispersions at 0.1 Hz and 10 Hz are shown in Table 6.1. Loss tangent values at 0.1 Hz compared and loss tangent of 0.5 wt% dispersant containing samples decreased from 11 to 6.4 during storage period while loss tangent of dispersant free dispersion decreased from 6.5 to 2.6 at the same period. Loss tangent decrement ratio of dispersant containing samples was lower during storage at 0.1 Hz. This was directly related with stabilization effect of adsorbed dispersant and prevention of agglomerate formation during storage.

Dispersions prepared with 0.5 wt% dispersant had lower loss tangent values at 10 Hz. Even there is no color strength measurement, from previous parts of this thesis, result of samples containing dispersant will have the highest color strength could be revealed. During storage period, 0.5 loss tangent increase was seen between dispersant containing samples at 10 Hz. This also showed color strength of samples stay close to be same during that period. Loss tangent at 10 Hz was decreased from 7 to 5.7 for dispersant free

dispersions. However higher G' value could be related with agglomeration of carbon black particles due to absence of dispersant. Color strength measurements weren't done due to possible effect of evaporation on results.

Table 3.1. Loss Tangent of dispersions during storage period

Samples	Loss Tangent	
	0.1 Hz	10 Hz
0 wt% D	6.5	7.0
0 wt% D (3M)	2.6	5.7
0.5 wt% D	11.0	1.0
0.5 wt% D (3M)	6.4	1.5

CHAPTER 7

CONCLUSIONS

Aim of this thesis was to investigate the rheological properties of carbon black inks and to determine their effect on color strength of printed films. The effects of pigment content, dispersant, varnish/solvent ratio, grinding medium, grinding time and storage period on rheological properties of carbon black inks were determined by both steady and dynamic shear measurements.

Rheological behavior of carbon black inks was determined by steady shear measurements. Most of the inks showed shear thinning behavior whereas only several inks showed shear thickening behavior at low shear rates and changed their behavior to shear thinning at higher shear rates. Dispersant content affected rheological behavior significantly. Dispersant free ink had higher viscosities than dispersant containing inks over the entire shear rate range and behaved shear thickening between range of 0.01 s^{-1}-0.18 s^{-1} beyond it was decreased from 13 Pa.s to 1.42 Pa.s in the range of 0.18 s^{-1} – 100 s^{-1}. Dispersant containing inks never exhibited thickening behavior and increase of dispersant content from 0.25 wt% to 0.75 wt% resulted in higher viscosities. Viscosity was increased and shear thinning behavior was observed at higher pigment contents. Higher varnish/solvent ratios increased viscosity of dispersions. Dispersions ground with 0.8 mm and 0.5 mm beads resulted in coarser and finer particle distributions respectively. Viscosity of dispersion with coarser particle size distribution was higher than dispersion with finer distribution. The effect of grinding time increase from 30 to 60 minutes on viscosity was investigated and no effect was determined at 20 wt% pigment contents. Increasing grinding time from 30 to 60 minutes caused higher viscosity at 25 wt% pigment contents. Storage of inks for 3 months period without dispersant showed viscosity increase while the viscosities of the inks containing 0.5 wt% dispersant stayed almost constant.

Dispersant content had a significant effect on thixotropy, and dispersant free ink showed 12 times higher thixotropy than dispersion with 0.5 wt% dispersant. Thixotropy area increased about 5 times with increase of pigment content from 25 to 30 wt%. Dispersions prepared with 2.2 V/S ratio had 679 $Pa.s^{-1}$ thixotropy while dispersions with

1, 1.29 and 1.67 V/S ratios had thixotropies of 432, 431 and 343 $Pa.s^{-1}$ respectively. Dispersion with finer particle size distribution had thixotropic area of $213Pa.s^{-1}$ while dispersion having coarser distribution had 1041 $Pa.s^{-1}$. Increasing grinding time from 30 minutes to 60 minutes with 25 wt% pigment content increased thixotropy from 324 to 1455 $Pa.s^{-1}$. Grinding time effect became negligible for dispersions with 20 wt% pigment.

Oscillation measurements were undertaken to determine G', G'' and loss tangent of inks. In general, G'' was dominant over G' which showed liquid like behavior. Dispersant free ink had lowest LVER and showed stress dependent behavior. Length of LVER was decreased with higher pigment content and varnish/solvent ratio increase. Grinding medium and particle size distribution effect on LVER was not observed for inks ground with 0.5 mm and 0.8 mm. Increasing grinding time extended LVER for inks prepared with 25 wt% pigment contents whereas LVER almost stayed constant for the 20 wt% pigment containing ink.

Relationship between rheology and color strength was investigated by loss tangent at 10 Hz. The results showed that dispersions with lower loss tangent had higher color strengths for 14 inks out of 16. The remaining 2 inks did not obey the inverse relationship between color strength and loss tangent and color strength difference with reference inks was only 0.68 % and 0.3 %.

Investigation of the rheological behavior of inks is necessary for the determination of the structure (particle-particle and particle-medium relationships) for developing new formulations and processes with higher application performances. In future, using parameters in this thesis or new experimental set-ups, determination of general rules that relates rheology and structural information is necessary to develop end used quality of inks.

REFERENCES

Agbo, C. W. (2017). A Review on the Mechanism of Pigment Dispersion. *Journal of Dispersion Science and Technology*.

Andersson, M., & Norberg, O. (2007). Color measurements on prints containing fluorescent whitening agents. *Color Imaging XII: Processing, Hardcopy, and Applications*.

Barnes, H. A. (1997). Thixotropy a review. *J. Non-Newtonian Fluid Mech.*(70), 1-33.

Barrie, C., Griffiths, P., Abbott, R., Grillo, I., Kudryashov, E., & Smyth, C. (2004). Rheology of aqueous carbon black dispersions. *Journal of Colloid and Interface Science 272*, 210-217.

E. N'gouamba, J. G. (2020). Yielding, thixotropy, and strain stiffening of aqueous carbon black suspensions. *The Society of Rheology*.

Faouzi Nsib, N. A. (2006). Selection of dispersants for the dispersion of carbon black. *Progress in Organic Coatings*, 303–310.

Frimova, A., Pekarovicova, A., Fleming, P. D., & Pekarovic, J. (2005). Ink Stability During Printing. *Taga Journal*, 122-131.

Hung-Wen Lin, C.-P. C.-H.-D. (2008). The rheological behaviors of screen-printing pastes. *Journal of materials processing technology*, 284–291.

Ibănescu, C., Danu, M., Nanu, A., Lungu, M., & Sımıonescu, B. C. (2010). Stability Of Disperse Systems Estimated Usıng Rheological Oscillatory Shear Tests. *Revue Roumaine de Chimie*.

Jia, X., Huang, B., & Wei, X. (2011). Study on the Influence of Rheological Properties on the Printing Quality. *Advanced Materials Research Vols 284-286*, 2018-2021. doi:https://doi.org/10.4028/www.scientific.net/AMR.284-286.2018

Kim, M. H. (2019). Effects of dispersion state on rheological and electrical characteristics of concentrated multiwalled carbon nanotube suspensions. *Korea-Australia Rheology Journal*, 179-186. doi:10.1007/s13367-019-0018-1

Luckham, P. F., & Ukeje, M. A. (1999). Effect of Particle Size Distribution on the Rheology. *Journal of Colloid and Interface Science 220*, 347–356.

Mewis, J., & Wagner, N. J. (2009). Thixotropy. *Advances in Colloid and Interface Science*, 214–227.

Mezger, T. G. (2014). *The Rheology Handbook 4th Edition.*

Mücke, R., Büchler, O., Menzler, N., Lindl, B., Vaßen, R., & Buchkremer, H. (2014). High-precision green densities of thick films and their correlation with. *Journal of the European Ceramic Society*, 3897-3916.

Nagose, S., & Rose, E. (2019). Study on wetting and dispersion of the Pigment Yellow 110. *Progress in Organic Coatings*, 55-60.

Norton, I. T., Spyropoulos, F., & Cox, P. (2011). *Practical Food Rheology An Interpretive Approach.*

Olhero, S., & Ferreira, J. (2004). Influence of particle size distribution on rheology and particle packing. *Powder Technology 139*, 69 – 75.

Oyarzún, J. M. (2015). *Pigment Processing Physico-Chemical Principles.*

Pal, L., & Fleming, P. D. (2006). The Study of Ink Pigment Dispersion Parameters. *The Hilltop Review.*

Péter Salamon, Y. G. (2020). Rheological and flow birefringence studies of rod-shaped pigment. *Journal of Molecular Liquids*.

R. Durairaj, S. R. (2009). Rheological characterisation and printing performance of Sn/Ag/Cu solder pastes. *Materials and Design*, 3812–3818.

R. Mücke a, O. (2014). High-precision green densities of thick films and their correlation with. *Journal of the European Ceramic Society*, 3897-3916.

R. T. Abrahao, V. P. (2013). Wettability study for pigmentary titanium dioxide. *J. Coat. Technol. Res.*, 829–840.

Schramm, G. (1998). *A Practical Approach to Rheology and Rheometry.*

Somalu, M. R., Brandon, N. P., & Yufit, V. (2011). A Study of the Rheological Properties of NiO/ScSZ Screen-Printing Inks and Their. *ECS Transactions*, *35*.

Tadros, T. F. (2010). *Rheology of Dispersions Principles and Applications.*

Thibert, S., J.Jourdan, B.Bechevet, & D.Chaussy. (2014). Influence of silver paste rheology and screen parameters on the front side metallization of silicon solar cell. *Materials Science in Semiconductor Processing*, 790-799.

Trefalt, G., & Borkovec, M. (2014). *Overview of DLVO Theory*. Retrieved from www.colloid.ch/dlvo

Weber, U. (2010). The Effect of Grinding Media Performance on Milling a Water-Based Color Pigment. *Chemical Engineering & Technology*, 1456 - 1463.

Woo, K. D. (2013). Relationship between printability and rheological behavior of ink-jet. *Ceramics International*.

Yasuko Saito, S. I. (2020). Suppressing aggregation of quinacridone pigment and improving its color strength by using chitosan nanofibers. *Carbohydrate Polymers*.